COMPREHENSIVE MATHEMATICAL ANALYSIS AND SIMULATION DESIGN OF A MICROWAVE WIRELESS POWER TRANSMISSION SYSTEM

By

Afrin Sultana Meem
16121084
Abrar Faisal
14121080
Pulok Tarafder
13321029
Bukenya Henry
15210002

A thesis submitted to the Department of Electrical and Electronic Engineering in partial fulfillment of the requirements for the degree of
Bachelor of Science in Electrical & Electronic Engineering

Department of Electrical and Electronic Engineering
Brac University
April 2019

Declaration

It is hereby declared that

1. The thesis submitted is my/our own original work while completing degree at Brac University.
2. The thesis does not contain material previously published or written by a third party, except where this is appropriately cited through full and accurate referencing.
3. The thesis does not contain material which has been accepted, or submitted, for any other degree or diploma at a university or other institution.
4. I/We have acknowledged all main sources of help.

Student's Full Name & Signature:

Afrin Sultana Meem 16121084	**Abrar Faisal** 14121080
Pulok Tarafder 13321029	**Bukenya Henry** 15210002

Approval

The thesis/project titled "*Comprehensive mathematical analysis and simulation design of a microwave wireless power transmission system*" submitted by

1. Afrin Sultana Meem 16121084
2. Abrar Faisal 14121080
3. Pulok Tarafder 13321029
4. Bukenya Henry 15210002

of Spring, 2019 has been accepted as satisfactory in partial fulfillment of the requirement for the degree of Bachelor of Science in Electrical & Electronic Engineering and Bachelor of Science in Electronic & Communication Engineering on 25th April 2019.

Examining Committee:

Supervisor:
(Member)

____

Dr. A.K.M Abdul Malek Azad
Professor, Department of Electrical and Electronic Engineering
Brac University

Program Coordinator:
(Member)

____

Dr. Saifur Rahman Sabuj
Asst. Professor, Department of Electrical and Electronic Engineering
Brac University

Departmental Head:
(Chair)

____

Dr. Shahidul Islam Khan
Professor, Department of Electrical and Electronic Engineering
Brac University

ABSTRACT

Wireless power transmission, an idea first proposed and demonstrated by Nikola tesla in the beginning of the 20^{th} century has seen immense improvement up until date, with the latest developments in the field including wireless charging of electronics having already graced the consumer market. In this paper, tremendous focus is put into improving the efficiency of the system, notably, the antennae efficiency, specific waveforms used to in transmission to achieve optimal efficiency. First, the non-uniform antenna array is designed and discussed. Additionally, mathematical analysis and software simulation designs of rectenna division, specifically, the rectifier part were performed. Consequently, a special type of rectifier known as the class F rectifier is discussed in detail simulated with different diode models to show the different improvements in the efficiency of the system depending on the type of diode used. Four waveforms were also compared, and simulation results given and compared to experimental results done in earlier work.

Dedication

This work is dedicated mainly to our parents for all their efforts and encouragement they have invested in us up until now. We also dedicate the work to our supervisor who has been more than a pillar in the development of the final work output.

Acknowledgement

We would like to thank our teachers, our supervisor and our friends who have been very supportive during the time of our work development. We would also like to thank our friends whose encouragement kept us going forward. And finally, each and every member of this team for having the dedication to work till the very end.

Table of Contents

List of tables

Table of figures

List of Acronyms

WPT	Wireless power transmission
MPT	Microwave power transmission
MWPT	Microwave wireless power transmission
LOS	Line of sight
PAPR	Peak to average power ratio
AC	Alternating Current
DC	Direct Current
EFI	Electric Field Intensity
PAA	Phased Antenna Array
LPT	Laser Power Transmission
OFDM	Orthogonal Frequency Division Multiplexing
Fig	Figure
EM	Electromagnetic
RMS	Root mean square

Chapter 1 Introduction

1.1 Background

Wireless power transmission dates way back to the beginning of the 20th century when it was first proposed by Nikola Tesla after which he successively demonstrated the idea through wirelessly lighting a bulb that he held in his hands at Colorado Springs laboratory. Up until date, rigorous research has been done in wireless power transmission both far and near field. Notably, near field techniques have been developed the most, with present-day implementations like wireless charging having already graced the consumer market, especially on the smart phone end. Consequently, now emphasis is being put into far field wireless power transmission research due to its promising outcomes which include but not limited to; transmission of power to remote or geographically poorly located places for example mountains or islands, where wired transmission would be difficult, the omission of power lost due to current flow in the conductor (I^2R losses), theoretically feasible way of transmitting harvested power from satellites to a station on earth without harming any bio elements passing through the line of sight between the satellite and the ground station. Currently, the approaches for far field transmission available include ***Laser power transmission*** and ***Microwave wireless power transmission*** (**MWPT**). In this paper, mathematical analysis and numerous simulations are to be presented in argument of improving efficiency of **MWPT.**

1.2 Literature review

[1] describes the work done in the field of ***wpt,*** the current trends both in far and near field techniques. The paper also throws light on the bottle necks still halting the development of the field especially in far field. Furthermore, the work elaborates on the various applications and importance of ***wpt.*** Experiments done in [2] demonstrated coupling of microwave RF power from using a magnetron and also simulation results from Multisim showed efficiency varying from 5.5% to 0.2%. Since having a high peak to average power ration is fundamental in the system to improve the conversion efficiency at the rectifying end, a great deal of work should be put into the type of waveforms used in the transmission. Therefore, [3] - [4] demonstrate with simulation results the different types of waveforms that can be used to provide better efficiency in ***wpt***. [3] further compares white noise signal waveforms, OFDM signal waveform, and Chaotic signal waveform and successively shows how chaotic signal has the highest PAPR amongst the three mentioned

waveforms thus theoretically promising the best conversion efficiency amongst them. Another keen area of interest in the system is the type of antenna used, both at the receiving and transmitting end. For that reason, very much work in recent years have been done to improve the antenna output. However, since the traditional antenna has a lot of challenges in transmitting power with a high directivity (for example, the size would be large according to the Friis transmission equation), more effort has been put into antenna arrays since they are more effective in increasing the directivity and gain without necessarily increasing the physical size of the antenna. Papers [5], [6] [7], [8], [9], [10], [14] discuss more on the antenna arrays. Finally, the rectification circuit to convert the received AC current to DC. For this case, tradition rectifying circuits struggle to handle the very high frequency signals and hence this work takes a deep look into the Schottky diode and the Class F rectifier. [11] discussed the different rectennas that can be used for microwave power transmission. [12]. The special Class F rectifier is discussed in [15] and [17].

1.3 Motivation

Today, a lot of causalities of electric shock are reported frequently and multiple fatalities like fire occur due to fault in electric transmission lines. However, this night mare can be omitted using wireless power transmission (**WPT**). Since there's no tangible means of transmission between the transmitter and the receiver, injuries occurring due to wires breaking or short circuits are easily eradicated in *WPT*. Additionally, *WPT* omits power loss due to current flow in a conductor (I^2R loss), provides a solution to transmit power to places with unfavorable geographical locations for example mountainous areas and Islands, among other advantages. Having come from countries with such major geographical barriers, that is to say, Uganda which is hilly and Bangladesh which has a lot of water sources, we got motivated to have a contributing hand in the sector promising to overcome the constraints we that cannot control (the geography). Thus, for the afore mentioned reasons, we take on this work.

1.4 Choice of Approach

Given the fact that significant work in near field ***wpt*** has already been done and even the technology availed to the end users, far field is the next destination for researchers hence our choice of approach. Far field today is being implemented in two major ways;

1.4.1 i) Laser power transmission

In this approach, power is beamed from a transmitter as laser light along a given line of sight to the receiving end. In the receiving end, light sensitive diodes are used which emit electrons when light of a given wavelength strikes their surface. In this way power is transmitted. However, the efficiency of laser power transmission is really low, and it also requires a clear line of sight and hence power transmission may easily be blocked in case there is an obstacle between the transmitting and receiving end. Thus, a need for a better or different approach.

1.4.2 ii) Microwave wireless power transmission (MWPT)

In the microwave approach, electrical energy is transformed to electromagnetic waves and transmitted along a wireless medium (channel) to a receiver which converts the received electromagnetic waves into electrical power specifically, direct current. ***MWPT*** currently provides the highest efficiency between the two far field techniques at 2.45GHz according to experiments. It also however has low efficiency at long distances thus the need for more work.

1.5 Over View of Entire Work

Introduction of the entire work flow of this paper and a brief history of wireless power transmission are covered in chapter 2. Chapter 3 discusses the antenna array both uniform and non-uniform. Then, chapter 4 discusses the methods that can be used to improve the efficiency of the channel. Chapter 5 covers the optimal waveforms to be used in the system for better rectification efficiency, followed by the discussion of the rectenna part, in particular, the class F rectifier covered in Chapter 6. Finally chapter 7 combines the entire system's contribution.

Chapter 2 Overall System Overview

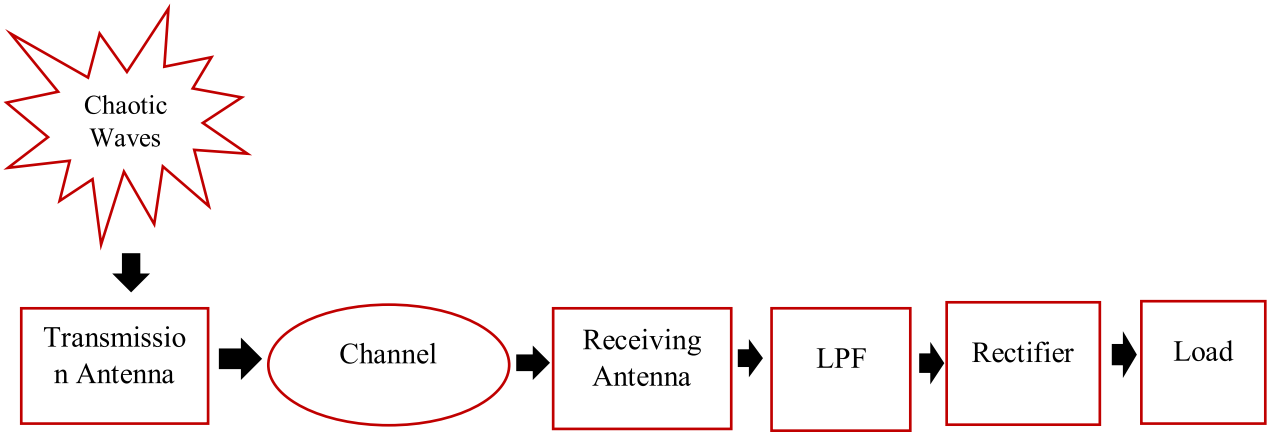

Fig. 2.1

2.1 System components

MPT has a lot of components that must be assembled to make it happen. To mention but a few, Antenna (both receiving and transmitting), signal fed to the antenna (in this case chaotic signal), amplifiers, filters, rectifiers at the receiving end energy converters (DC to DC converters for the system in question), the channel characteristics have to also be taken into consideration to reduce the distortion of the signal received, and finally the load or energy storage device like a battery. In this work, we focus mainly on the major part of the system that include;

1. Input signal, that is, Chaotic signal
2. Channel efficiency
3. Transmitting and receiving antenna
4. Rectifier (Class F rectifier)

2.2 Input Signal

A great deal of scrutiny must be put in the choice of signal to be used in ***MPT*** because; 1) we are dealing with microwave frequencies thus a lot of electrical properties of electrical and electronic devices change. 2) The signal has to be transmitted through free space where characteristics of the wireless transmission line cannot be predicted to perfection. For the afore mentioned reasons, much research is done today about the signal to be used in the ***WPT*** systems. In this work, we take a deeper look at signals with a high ***peak to average power ration*** (***PAPR***). These include white noise, OFDM, and chaotic waveforms. The roles of high ***PAPR*** are discussed in chapter 4. However, with these three signal waves forms analyzed as shown in [3] and [4], chaotic waveforms are the most promising ones in giving the required ***PAPR*** thus our choice of choosing these for our system. Fig. 2 shows an example of a signal with high ***PAPR*** specifically ***OFDM*** signal.

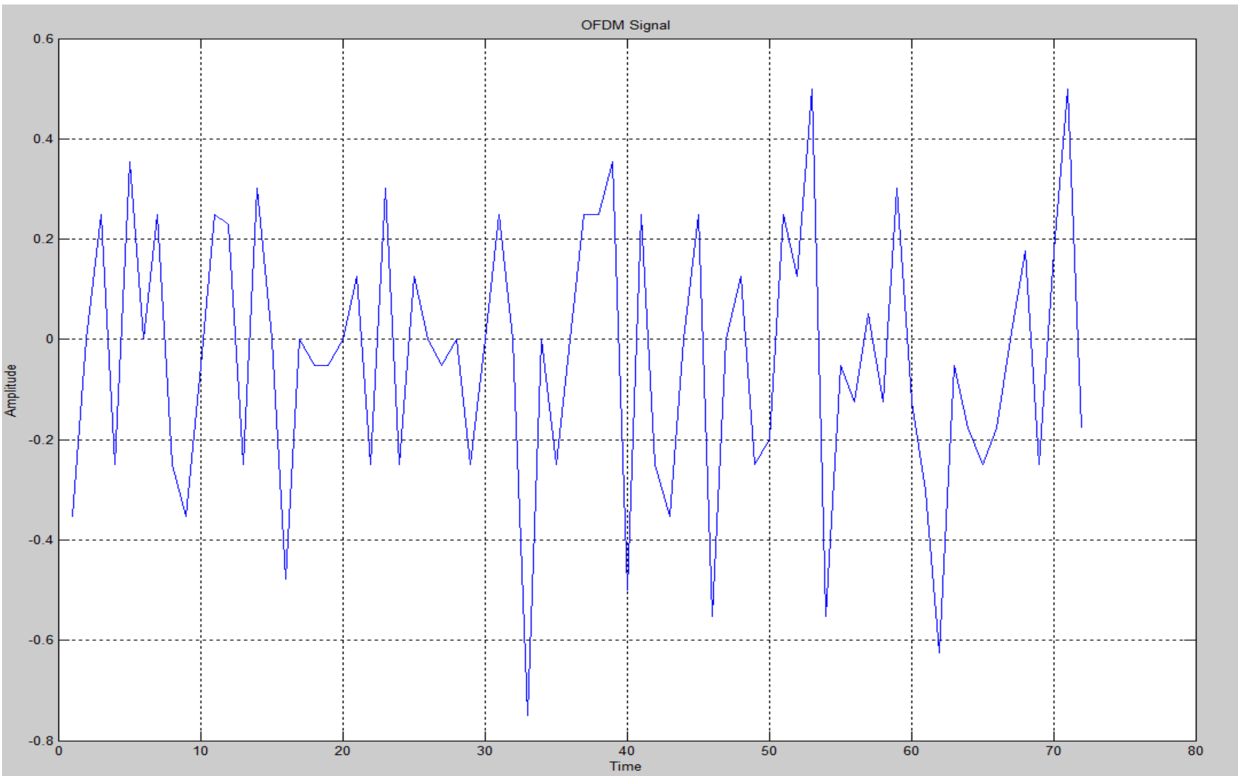

Fig. 2.2 OFDM signal waveform

2.3 Channel efficiency

The channel is the medium linking the transmitting antenna to the receiving antenna. In case of ***WPT***, the channel is the wireless free space (ideal condition) between the transmitter and receiver. The efficiency of the channel can be calculated using the Friis transmission formula (1) as described in chapter 4. With the equation's dictation, few methods are available to increase the efficiency of the channel, that is, increasing transmission frequency, increasing the aperture of either one of the antennas, finally decreasing the space between two antennas. In this work, we choose the increase of frequency due to reasons described in chapter 4. [6]

2.4 Transmitting and receiving antenna

Antenna choice is fundamental to successful transmission and reception of signals in any wireless system. Therefore, in chapter 2, different antenna types are given henceforth selecting a desired one for this work as the antenna array coupled with beam steering technology due to its size advantage and ability to change the direction of the output beam without physically adjusting the antenna, thus making it a good choice for satellite power harvesting and transmission to a base station on earth. Then non-uniform rectenna array as discussed in [13] is simulated and also same idea simulated for the transmitting antenna in this work. Conclusively, the detailed work on antennas is in chapter 2.

2.5 Rectifier

One of the principal parts of the receiving side of the system is the rectification part (rectenna). It is mainly tasked with conversion of the received signal to direct current which is then used as desired. We examine the Class F rectifier where also simulation of the efficiency of the rectifier designed with various diodes and fed with different power in milli Watt (mW) range is done. The diode choices matter since in ***MPT*** electrical properties and thus traditional silicon diodes can not keep up with the very high frequencies. The results and details of the rectenna work are discussed in Chapter 5.

Chapter 3 Antenna

3.1 Introduction

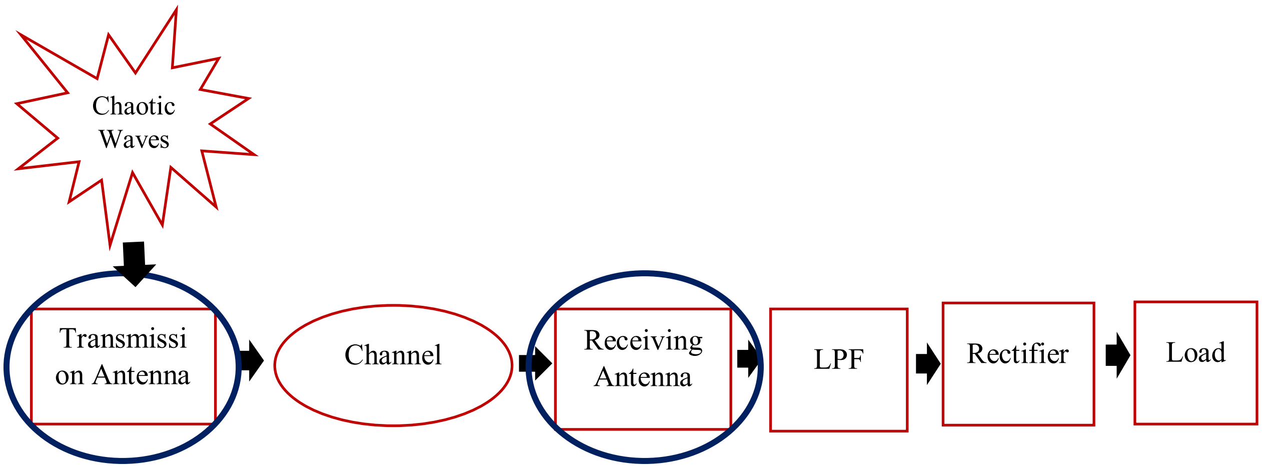

Fig. 3.1 Receiving and transmitting antenna

The standard definition of Antenna as given by IEEE in The *IEEE Standard Definitions of Terms for Antennas* (IEEE Std 145–1983), states that the antenna or aerial is "a means for radiating or receiving radio waves". In other words, an antenna is a means of converting guided electrical energy into free space radio waves. The Antenna is a salient component of any communication system that involves sending signals over free space since it does the conversion of electrons to photons at the transmitter and does the vice versa conversion at the receiver.

In order to have a good communication system, be it a ***WPT*** system, much emphasis has to be put into designing the antenna. For example, if the antenna is improperly designed, the standing waves formed in the transmission line due to constructive and destructive interference may store more energy, leading to the transmission line acting more like an energy storage medium than an energy transmission medium. Consequently, this effect may have a lot of disadvantages one of which is; if the ***EFI*** in the standing waves is too high, arching in the transmission line may occur. Hence, the need to design the antenna with precision and much thought is inevitable.

3.2 Antenna Types and their advantages over one another

I. **Wire antenna**. A finitely long, in either a dipole form, loop, or Helix is used. Its strong point is that it has a simple construction mechanism. An example of the wire antenna is shown in Fig. 3.2 below.

Fig. 3.2 Wire antenna

II. **Aperture antenna**; Usually employed in space and aircraft work due to their easiness of getting mounted to the plane's surface. Examples Horn Antenna (shown in Fig. 3.3).

III. **Microstrip antenna**; Grounded substrate with metallic substrate. Can be applied in places with very small spaces and also be easily printed on circuit boards.

IV. **Reflector antenna**; Shown in Fig. 3.4, this is employed for long distance transmissions.

V. **Antenna array**; In this case, small types of antennas mainly patch antennas (Fig. 3.5). The main advantage is, the direction of the beam can be adjusted using an electrical signal (by varying the delay in individual signals reaching each of the antenna slots).

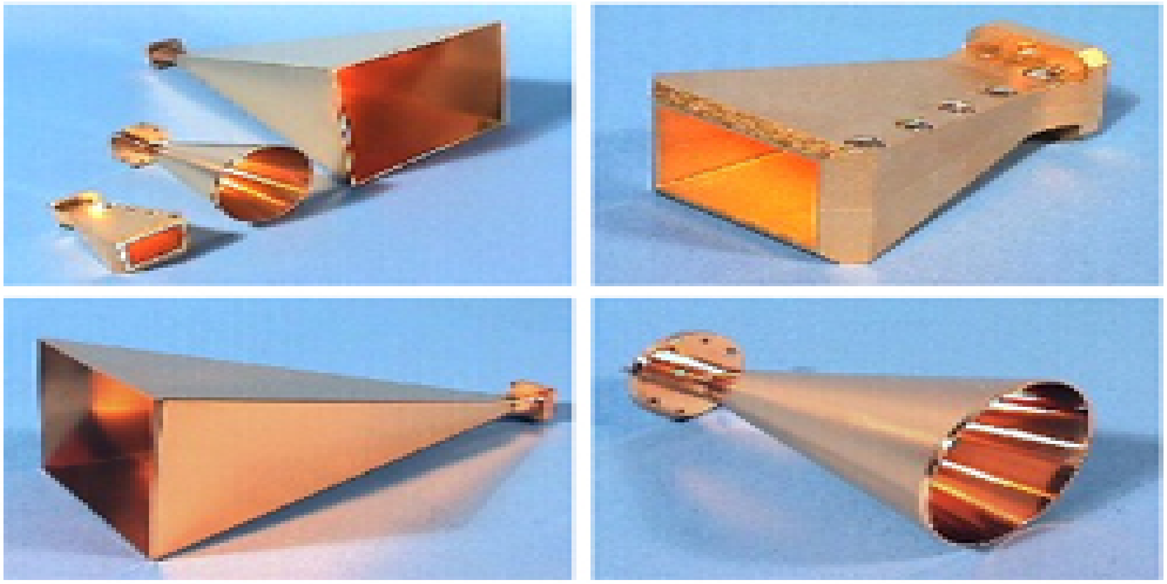

Fig. 3.3 Aperture antenna

Fig. 3.4 Reflector antenna

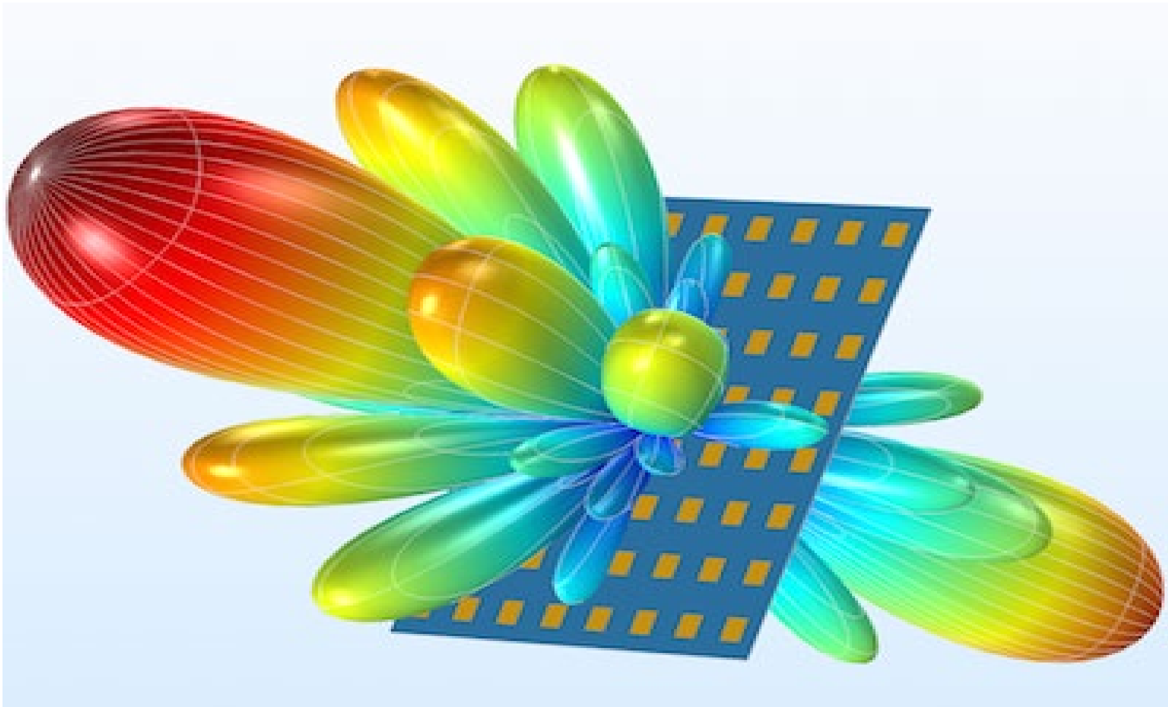

Fig. 3.5 Antenna Array

VI. **Lens antenna**; used to transform divergent or convergent signals into plane waves and vice versa.

Fig. 3.6 Lens antenna

Note: **The main goal of antenna design is to make sure it radiates all the power fed to it** [14].

3.3 Choice of Antenna

In microwave wireless power transmission, the power transmitted in a desired direction is a big factor. Additionally, since one of the major objectives of this research is to make sure users can receive power while even in motion and satellites transmitting power direct to earth, then directivity of the antenna is very much important. As deduced from the *Friis transmission equation* (3.3.1) shown below, attaining a highly directive antenna as required in ***WPT*** applications would require a large aperture of the antenna meaning a very large antenna which would in-turn be tough to move physically in order to change direction of the output signal and very expensive to propel into the orbit.

$$\frac{P_r}{P_t} = \frac{A_t\ A_r}{R^2\,\lambda^2} \tag{3.3.1}$$

However, antenna arrays give a viable alternative to this headache of size since they can be printed of a patch and mounted on the surface of the device to be used. Additionally, the ability to control the direction of the signal electrically is as important. Therefore, in this work we select to use the ***Phased Antenna Array*** due to its very aspect of controlling the direction of its output depending on an electric signal. In this way, a control station on earth can be able to direct the output beam from a satellite thousands of miles away without having to physically get to the satellite or even change its physical tilt since this may consequently affect its functionality and also call for more complex calculations and costs to be incurred. Additionally, since the main goal for ***MPT*** is power delivery, another main concern of the antenna is the power it outputs. In this case, if we use one large antenna to transmit all the power, the electrical components to feed it with such large amounts of power at these very high frequency (in this case 2.45GHz) may not be efficient enough if they are available at all. In this regard, the antenna is divided into smaller potions which are fed directly with smaller inputs each, as compared to one large antenna thereby giving the final output power as an aggregate summation of the individual small antenna elements' outputs. This eases the electrical load on each of the elements resulting in advantages like reduction in heat generation, increase in overall efficiency, to mention but a few.

3.4 Beam steering technique

3.4.1 How beam steering works

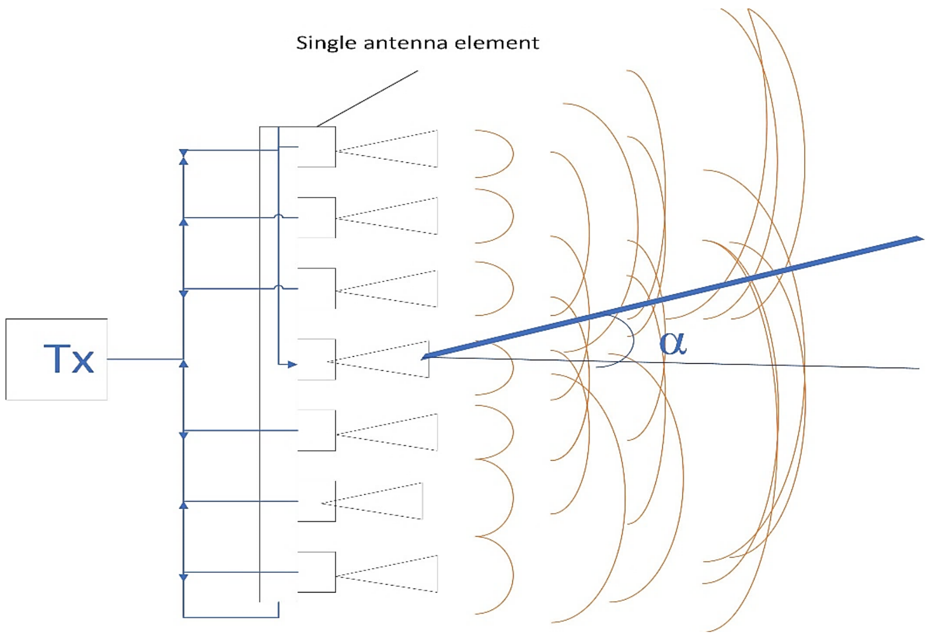

Fig. 3.7 Beam forming by an array of antennas

The signal sent to each of the elements is delayed by a certain factor and consequently, due to constructive and destructive interference, a reinforced beam is formed in a given (preset by the system designer) direction as shown in Fig. 3.7 above.

This beam's direction can then be adjusted accordingly by changing the delays furthermore. This can be effectively advantageous if the gadget being powered by the system wirelessly is in motion. Therefore, this is the main reason phased antenna array outweighs the other antennas in ***MPT***.

3.4.2 3D representation of the output beam

Fig. 3.8 shows how the 3D radiation pattern varies with change in the distance between the elements (individual patches in the array). When the distance, is too large, the output beam is very scattered and is not strong in any given direction. However, the individual lobes have very high gain. As the distance reduces, the beam starts to converge as shown in the figure and it strengthens

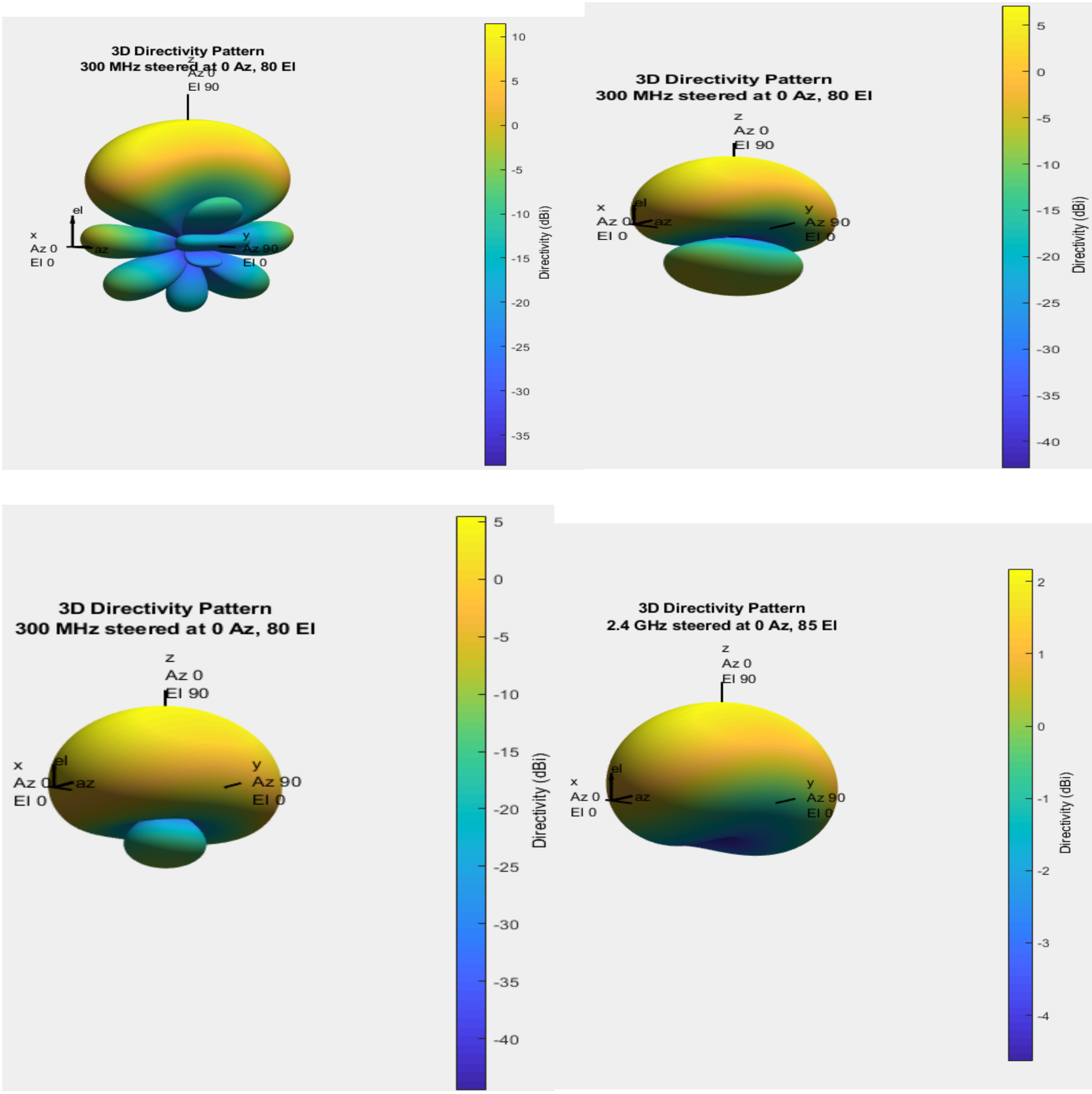

Fig. 3.8 Radiation pattern change as distance between the elements is reduced

in a given direction as dictated by the designer through the feeding delays. As the beam spreads out, to form a one large the maximum gain reduces as evident in the simulation results above. This is compensated by the fact that now someone in the near vicinity of the antenna will not easily lose connection since the beam is well spread and somewhat continuous.

3.5 Antenna design and simulation results

Using MathWorks' MATLAB antenna designer software, a 64-element array was designed to demonstrate the beam steering technique. Simulation results are shown below (Fig. 3.9). Az refers to the horizontal sweep while El refers to the vertical sweep.

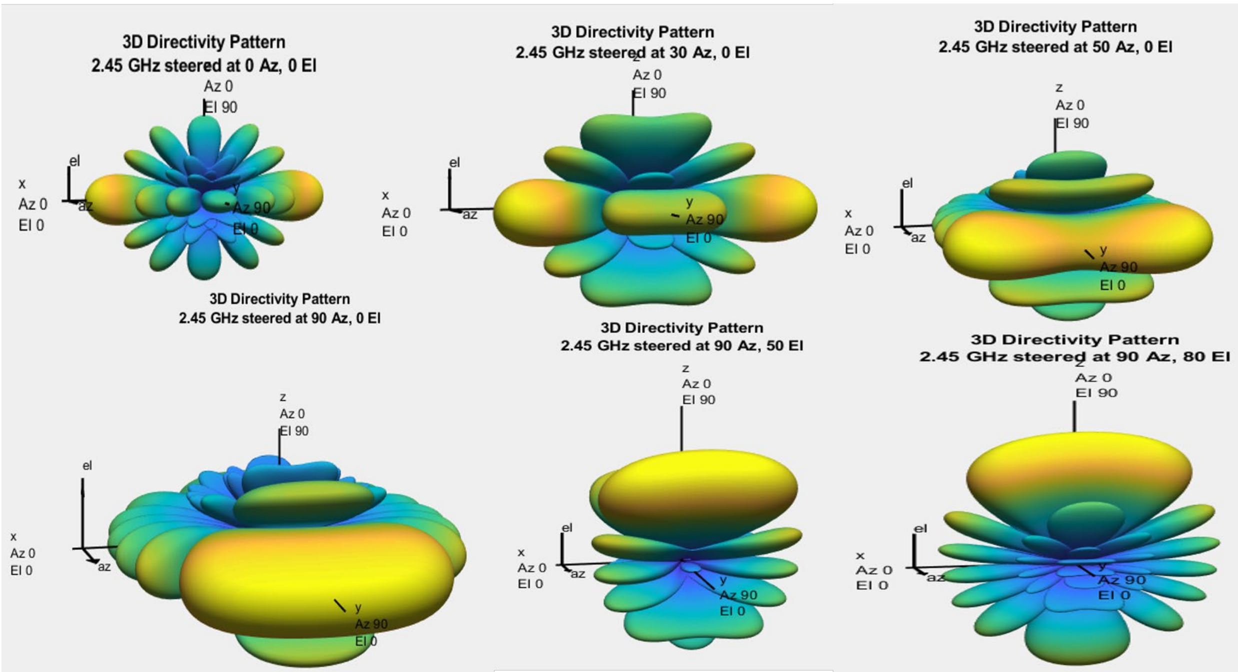

Fig. 3.9 Beam steering technique 3D representation shown in matlab

3.6 Simulation model

In this work, an array (3x3) was designed in **ANSYS HFSS** for two case scenarios as will be explained below. The goal of this approach was to compare the route proposed in [13] of using non-uniform rectenna array to improve the efficiency of a ***WPT*** system. First a single rectangular patch was designed and simulated which was later transformed into a uniform 3x3 rectangular array thereafter comparing the two results. Furthermore, the 3x3 rectangular array was transformed into a non-uniform array by replacing the middle line of the array with circular patches. Consequently, the results were analyzed, and a detailed report is given in section 3.7. The models were as follows;

3.6.1 Single rectangular patch array at 28GHz

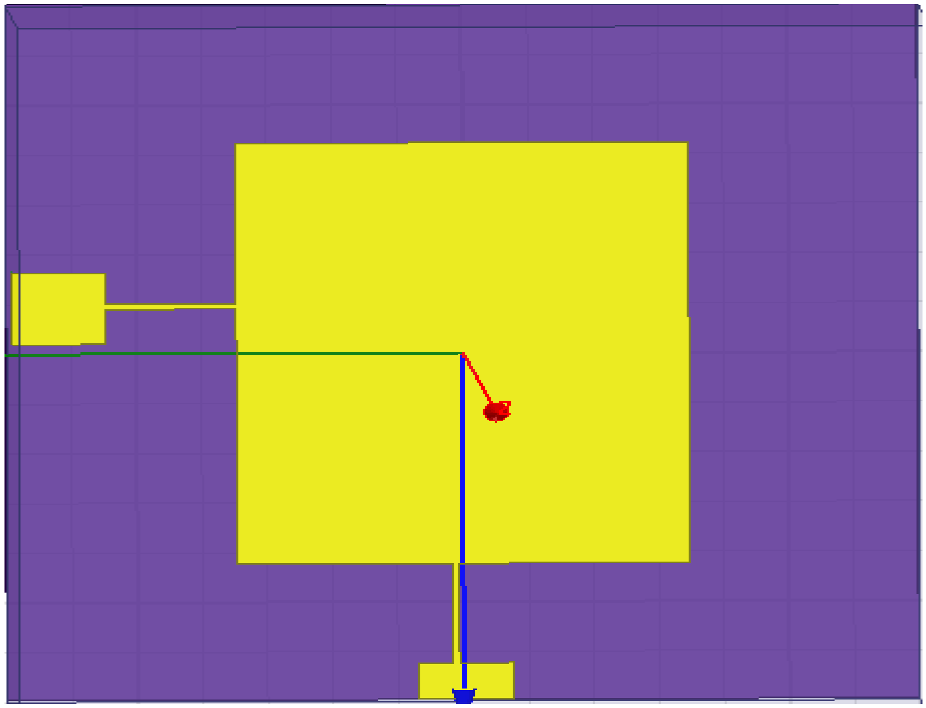

Fig. 3.10 Single rectangular patch at 28GHz

As shown in Fig. 3.10 above, the single patch had dimensions as follow;

Lp = 3.47mm

Wp = 4.235mm,

Where Lp is the length of the patch and Wp is the width of the patch. The dimensions mentioned where calculated from the following formula.

$$W_p = \frac{C}{2f_r\sqrt{\frac{\varepsilon_r + 1}{2}}}; \qquad (3.3.2)$$

And

$$Lp = \frac{c}{2f_r\sqrt{\varepsilon_{eff}}} - 0.824h\left(\frac{(\varepsilon_{eff} + 0.3)\left(\frac{W_p}{h} + 0.264\right)}{\varepsilon_{eff} - 0.258\left(\frac{W_p}{h} + 0.8\right)}\right) \qquad (3.3.3)$$

Where

$$\varepsilon_{eff} = \frac{\varepsilon_r + 1}{2} + \frac{\varepsilon_r - 1}{2}\left[\frac{1}{\sqrt{1 + 12\left(\frac{h}{w_p}\right)}}\right]$$

Where f_r is the resonant frequency, ε_r is the dielectric constant and h is the height of the substrate. The higher the h value, the better. $\varepsilon_{r\ value}$ chosen was 2.2 as used in [15] with a substrate (Rogers RT/duroid 5880) height of 0.25mm due to narrow bandwidth used.

3.6.2 3x3 rectangular array

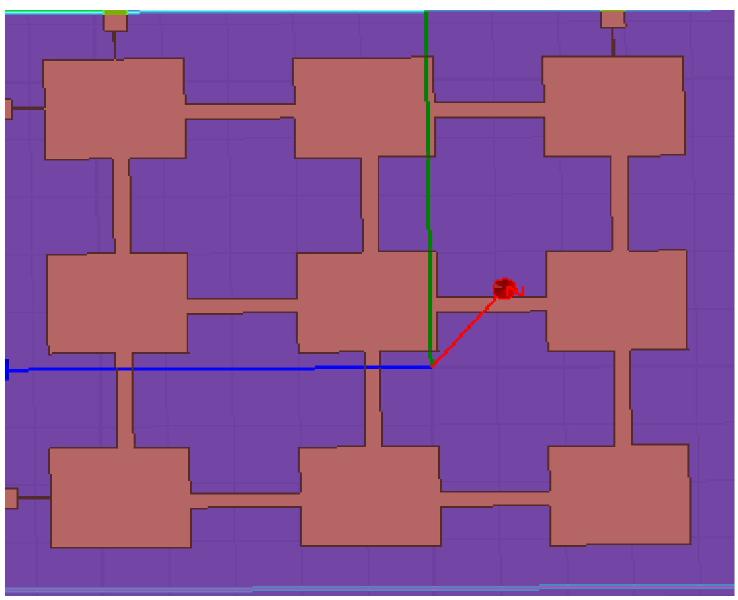

Fig. 3.11 3x3 rectangular array designed with HFSS

Shown above is the rectangular array. The array is fed using a four-port series feed. If Ls is the length of the line connecting to successive patches together and Ws the width of the line, according to [15], the optimal values for Ls and Ws are 3.3mm and 0.5mm respectively. However according to our simulation results, the optimal results, notably those for the reflection co-efficient were obtained at Ls = 3.6 as shown in Fig. 3.17 below.

3.6.3 3x3 non-uniform patch array

The array shown above in Fig. 3.13 depicts the 3x3 non-uniform array designed in this work to compare with the 3x3 uniform rectangular array. This array was also analyzed for Ls values and as evident from the graph in Fig. 3.18 the design has an optimized performance at Ls = 3.6mm and 3.8mm. Here, the trick part was to determine the radius, a, of the circular patch to be used. According, to the specifications of substrate height (0.25mm), dielectric constant (2.2) at 28GHz the radius which is given by the standard formula below

$$a = \frac{F}{\left\{1 + \frac{2h}{\pi \varepsilon_r + F}\left[ln\left(\frac{\pi F}{2h}\right) + 1.7726\right]\right\}^{1/2}} \qquad (3.3.4)$$

where

$$F = \frac{8.791 \times 10^9}{f_{r\sqrt{\varepsilon_r}}}$$

$$a_e = a\left\{1 + \frac{2h}{\pi \varepsilon_r a}\left[ln\left(\frac{\pi a}{2h}\right) + 1.7726\right]\right\}^{1/2} \qquad (3.3.5)$$

Where f_r is the resonant frequency.

However, using formulas (3.6.4) and (3.6.5), the values received are a = 0.162mm and a_e = 0.2173mm which are way smaller than the line width of the line separating the patches. Hence using these values would not be practical at all. For this reason, three options of radius were chosen and those depend on the rectangle dimensions as shown Fig. 3.12. Using Pythagoras theorem, the radii are;

R_1 = 2.117mm, R_2 = 2.737mm and R_3 = 1.735mm. R_3 was so large and gave unconverging results for the gain, R_2 was so small and the circle could not reach some of the feedlines therefore, R_1 was the best option as it gave the best results with also the highest stability values.

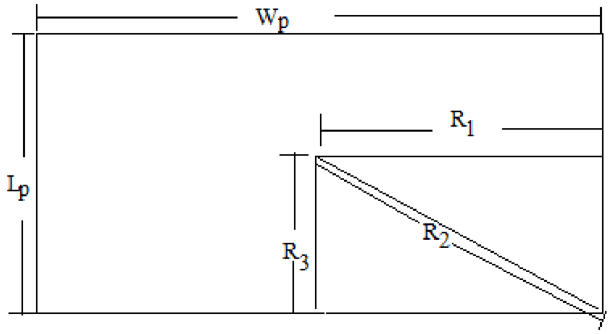

Fig. 3.12 Patch dimensions with radius options

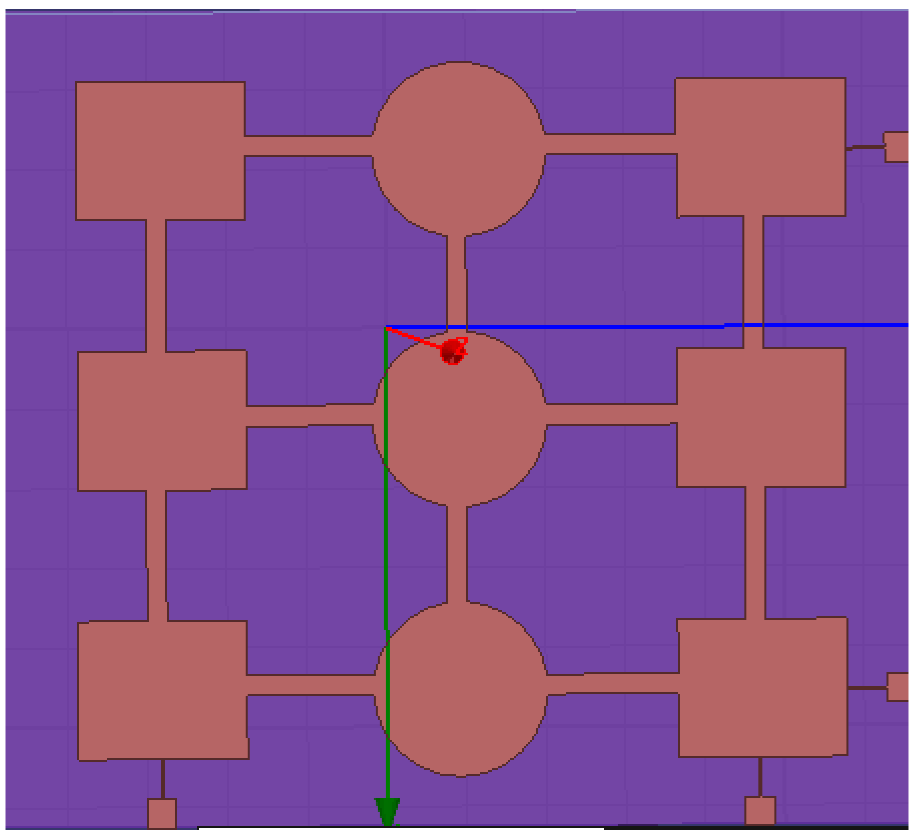

Fig. 3.13 3x3 non-uniform array designed in HFSS

3.7 Results and discussion

The single patch antenna gave a high maximum gain of up to 6dB as well as the directivity (considering a lot of ideal factors such as perfectly conducting patches) as shown in the Fig. 3.14. The side lobs are also not as many.

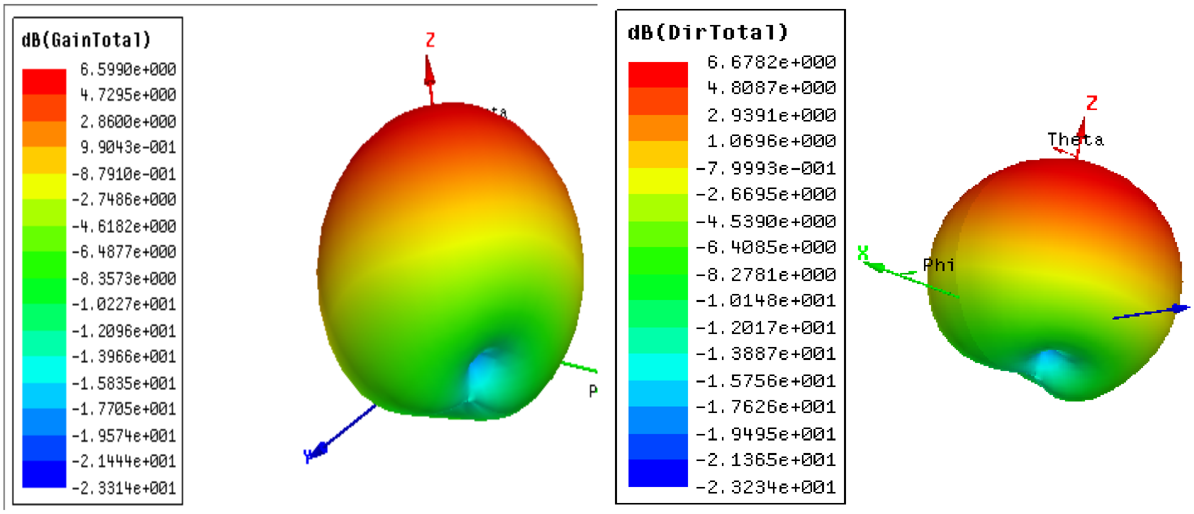

Fig. 3.14 Gain (left) and directivity (right) 3D polar graphs for single patch

The gain for the 3x3 patch at Ls = 3.3mm is higher than that given by the single patch peaking a 7dB (Fig. 3.15) as compared to 6dB from the single patch this is shown in Fig. 3.14, and the directivity of the uniform array is still high with a maximum peaking at 7.46dB which is also higher than that of the single patch.

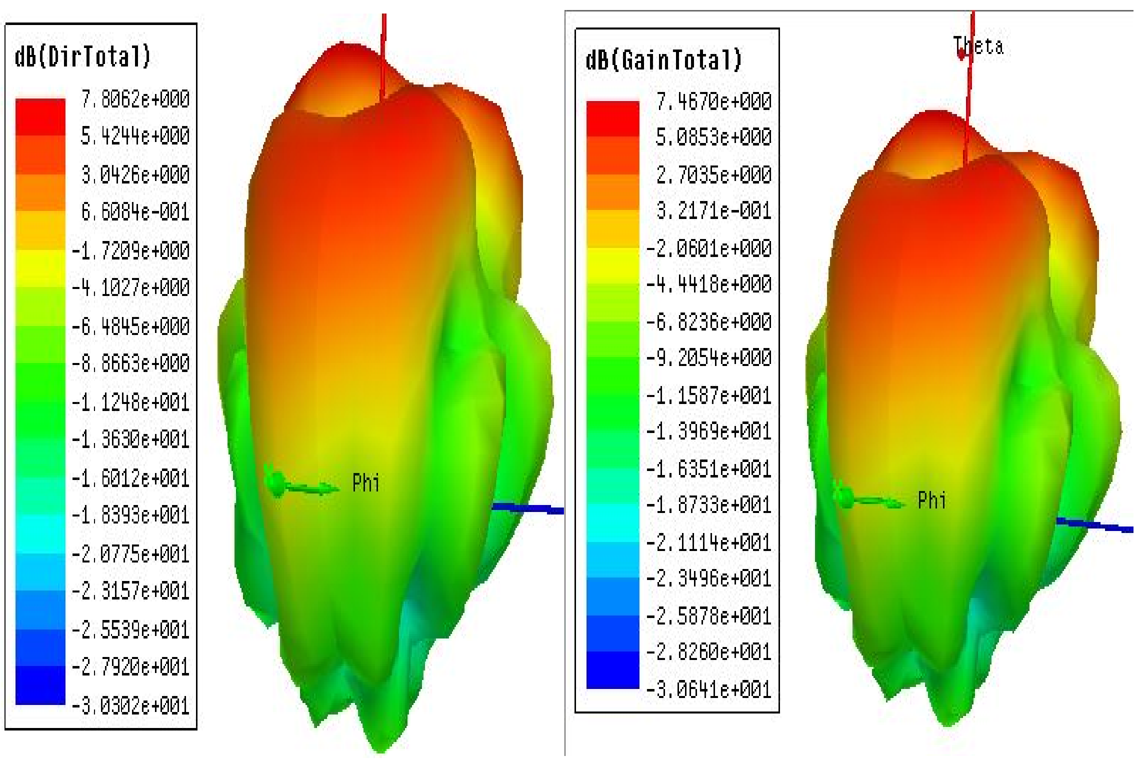

Fig. 3.15 Gain (left) and directivity (right) of 3x3 rectangular array

This is because the radiation of the array is an aggregate summation of the individual lobes from each of the patches (single ones) that make up the array. The direction of the beam can, to a high degree also be adjusted electrically.

Fig. 3.16 below shows the 3x3 non-uniform array. As evident from the graph, the non-uniform array gives a higher gain than both the uniform array and single patch. It has a maximum peak of 9.06 dB for the directivity and 8.8 for the gain. Thus, giving better results which is in line with this paper's argument of non-uniform array giving a better performance.

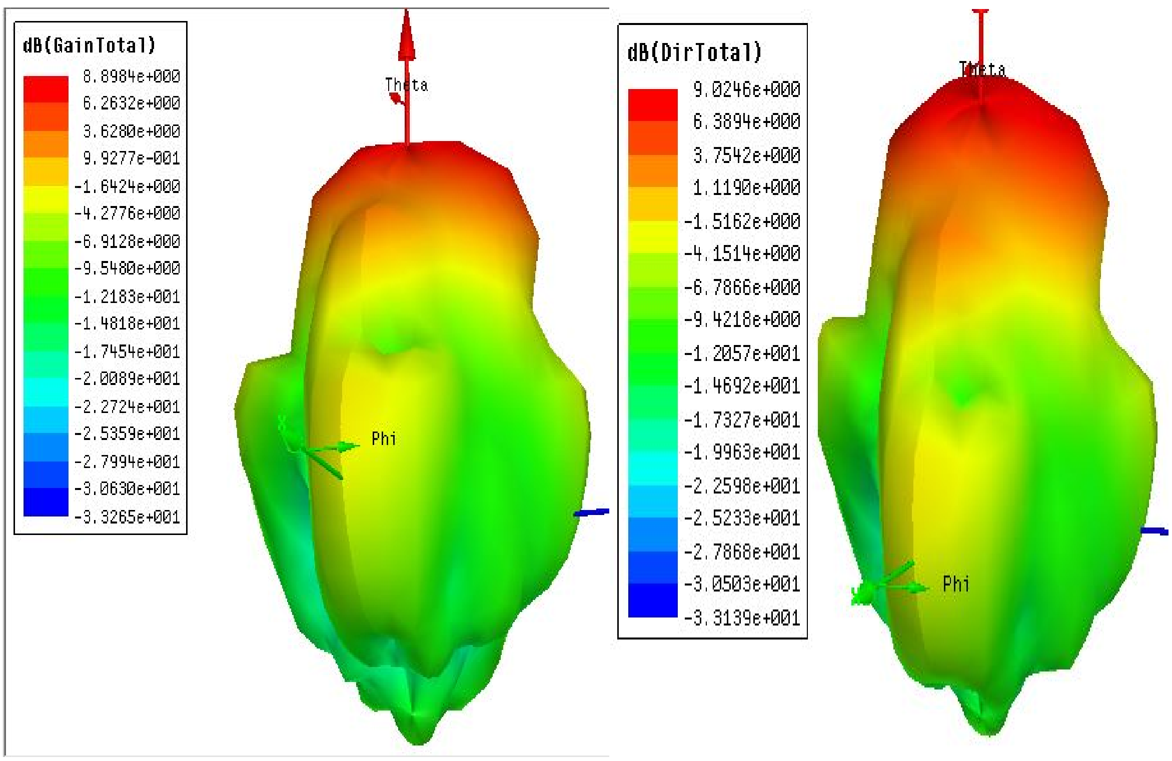

Fig. 3.16 Gain (Left) and directivity (right) of a non-uniform array

The S(1,1) parameter's graph is shown below with various separation distances. Fig. 3.17 shows S(1,1) of the uniform rectangular array and Fig. 3.18 shows that of the non-uniform one. At nearly 28GHz, the uniform array gives slightly better performance since it has a lower peak for the reflection co-efficient with Ls = 3.6mm. Nevertheless, the non-uniform array outcompetes the uniform one when it comes to consistence as Ls values changes (between 3.4mm to 3.8mm), this means that slight errors during manufacturing that may cause small variation in the Ls value will not drastically affect the reflection of the power. Thus, the non-uniform may be better for real life application.

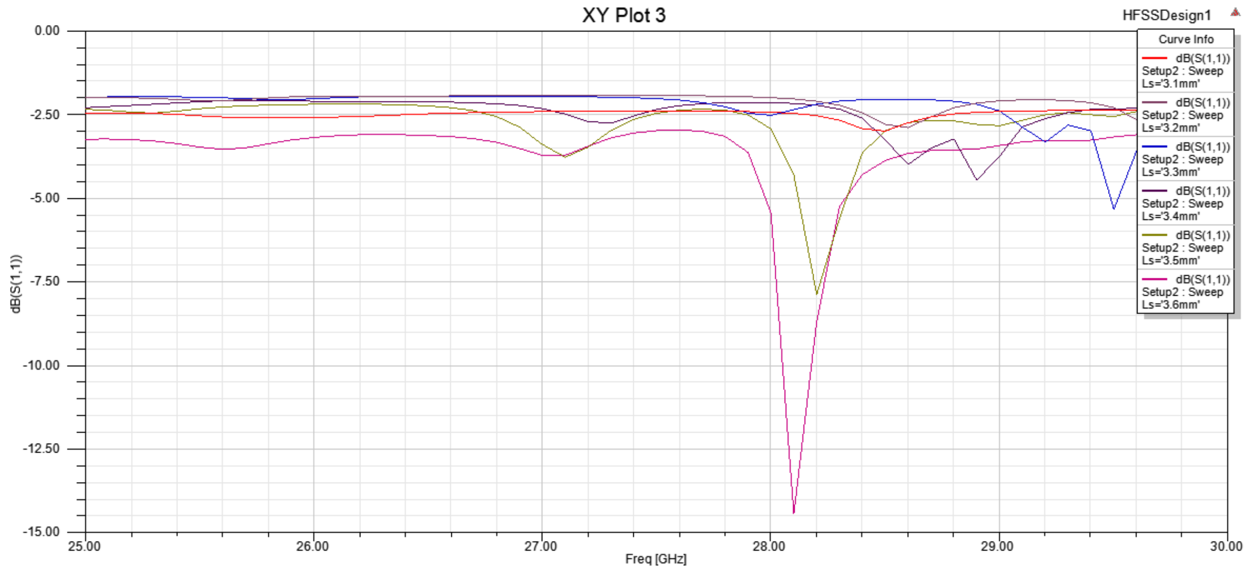

Fig. 3.17 S(1,1) output graph for different values of Ls for a 3x3 rectangular array

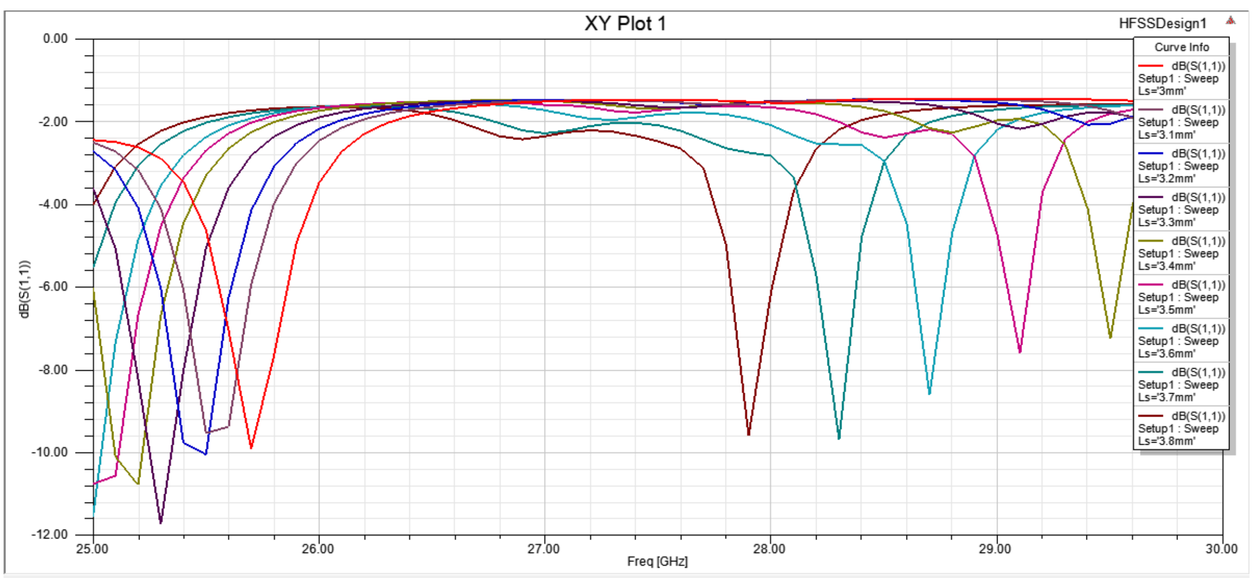

Fig. 3.18   S(1,1) parameter for 3x3 non-uniform array simulated in HFSS

Chapter 4 Channel efficiency

4.1 Introduction

In this following area of research, calculating the power of antenna is one of the fundamental criteria to ensure channel efficiency. The Friis transmission equation shows the relation between received power and transmitted power, distance between two antennas and gains of the link. Optical geometry theory and parameters used in antenna design were used to come up with this formula. Since the equation is based on optical radiometry it uses areas, aperture and angles to find the amount of power transmitted by an electromagnetic wave. In the field of engineering like telecommunication, the Friis transmission formula has been used by equating the power at the terminals of a receiver antenna as the product of power density of the incident wave and the effective aperture of the receiving antenna under idealized conditions given another antenna is some distance away transmitting a known amount of power. In this chapter we have used Friis transmission equation for the channel between two antennas to deduce some method to that will improve efficiency of the system. The equation (3.3.1) is section 3.3.

The descriptor of antenna capture area is one of two important parts of the transmission formula that characterizes the behavior of a free-space radio circuit. From Fig. 4.1, an isotropic antenna is considered, and the receiving antenna has an effective area of A_r with R being the distance between the antennas.

As stated by Friis, the point where this formula out ways the others is the absence of numerical coefficients to remember though does require transmitting antenna's performance expression as a function of power flow per unit area instead of field strength plus the receiving antenna's performance expression as a function of its effective area instead of its power gain or radiation resistance [16].

The effective antenna area is a theoretical value which is a measure of how effective an antenna is, at receiving power. The effective area can be calculated by knowing the gain of the receiving antenna. The effective area of an antenna is defined for the condition in which the antennas used to reach a linearly polarized electromagnetic wave. The antenna efficiency is given as;

$$A_{eff} = \frac{Pr}{Po} \quad (3.3.6)$$

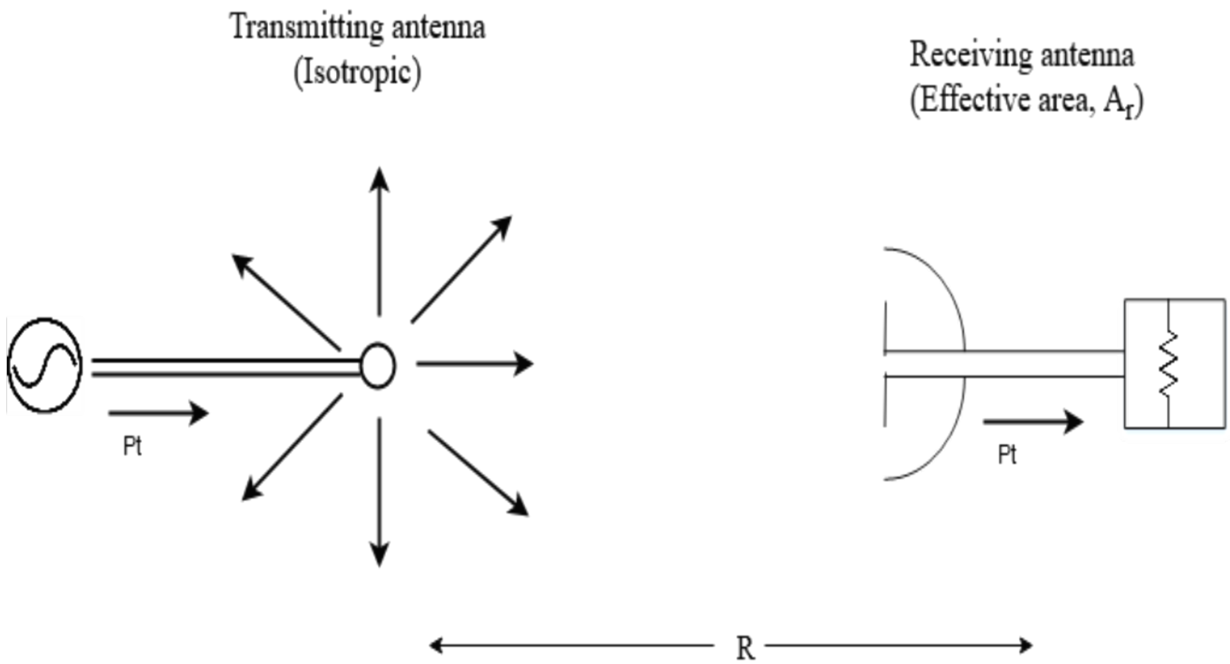

Fig. 4.1 Friis free space radio transmission system's block design

4.2 Methods for improving the antenna efficiency

The main aim of this chapter is to formulate a way to increase the efficiency of the system especially in the channel. There are a couple of methods available that can be applied to increase the channel efficiency. Based on Friis transmission equation there are several ways to obtain higher channel efficiency which include; changing channel frequency, increasing the antenna aperture and reduction of the distance separating the antenna.. Brief description of the effective ways are as follows,

4.2.1 Increasing the transmission antenna aperture

If the aperture of any antenna has been increased, then the channel efficiency is expected to increase accordingly. Increasing the aperture of any antenna increases output the beam of that antenna which ensures more power from electromagnetic field thus improving overall efficiency.

Using the isotropic gain, G, any antenna's ability to direct radio waves in one direction or to receive from a single direction can be measured. Mainly the isotropic gain, G, is the ratio of the power, P_o, received by the antenna to the power, P_{iso}, that would be received by a hypothetical isotropic antenna which receives power equally well from all directions. It can be seen that the gain is also equal to the ratio of the apertures of these antennas.

$$G = \frac{\mathrm{Po}}{\mathrm{Piso}} = \frac{Ae}{Aiso}$$

The aperture of a lossless isotropic antenna, which has unity gain, is

$$Aiso = \frac{\lambda^2}{4\pi}$$

Where, λ is the wave length of the radio waves. That is why,

$$G = \frac{Ae}{Aiso} = \frac{4\pi\ Ae}{\lambda^2}$$

And, for an antenna with a physical aperture of area, A_{phys},

$$G = \frac{4\pi\ \mathrm{Aphys}\ ea}{\lambda^2}$$

Therefore, antennas with large effective apertures are high gain antennas. However, it has some limitations. We know any antenna having larger antenna aperture, can collect more power from electromagnetic field. In addition to that, this is a function related to the direction of electromagnetic wave and the antenna radiation pattern. If we want to increase the antenna aperture we will need bigger size antennas which has widespread beam. That can be acceptable for transmitting side but not for receiving antennas. In that case, there will be wastage of electromagnetic waves at the receiving end due to smaller beam of receiving antenna [17].

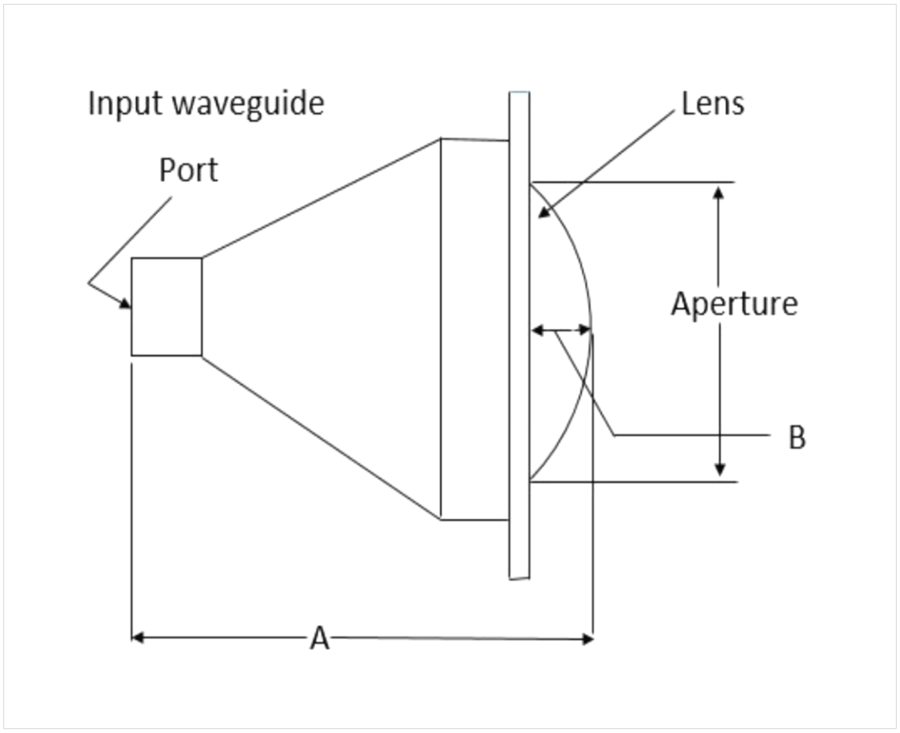

Fig. 4.2 Effective aperture of a transmission antenna

4.2.2 Increasing the receiving antenna aperture

The second method from the Friis transmission theory is increasing the receiving antenna aperture. If the four methods are compared it can be found that it is one of the most efficient methods for increasing efficiency, theoretically. If we look into the given equation,

it can be seen that if aperture is increased in the receiving end, we can get more power. To increase antenna aperture in the receiving end, again, we need bigger size antennas which is complicated in nature, expensive and has multiple drawbacks related to antenna beam and radiation patterns. The purpose of the receiving antenna is to enhance the reception of a signal in a direction relative to other directions to minimize interference and noises from other signals. To obtain this type of antenna characteristics in the receiving end, the antenna must be in a specific size range but we cannot increase the aperture without increasing the antenna size. So, in this paper we are proposing the use of phased array antennas which is basically a group of small antennas. In antenna theory, a phased array usually means an electronically scanned array, a computer-controlled array of antennas which creates a beam of radio waves that can be electronically steered to point in different directions without moving the antennas. It can be used for higher efficiency and it will be smaller in size as well.

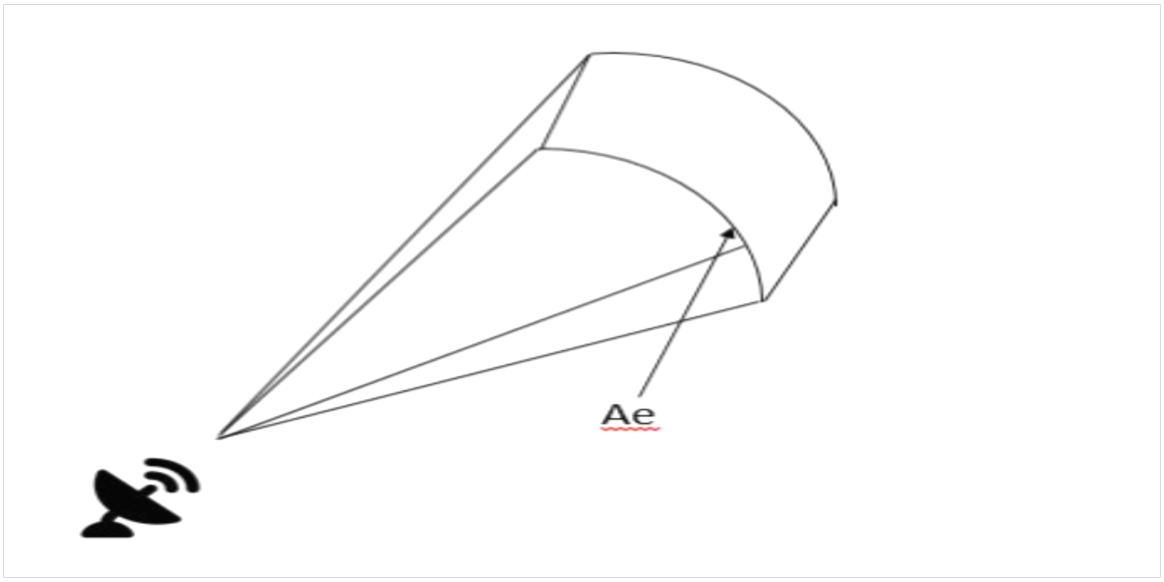

Fig. 4.3 Effective aperture of antenna beam

4.2.3 Reducing the distance between antennas

There are some other ways to transmit power which is by using magnetic resonance and inductive coupling, but their range is very short. For our case, reducing distance will not be considered since our main goal is radio frequency based far field transmission. Based on electromagnetic field regions and their interactions we can define 'Near field' and 'Far field'. We cannot reduce the distance between two antennas but to justify the far field phenomena we can look into some mathematical calculations. If we look into this equation,

$\lambda = c/f$

$= (3.00 \times 10^8)/(2.45 \times 10^9)$

$R = \lambda/2pi$

$R=0.122/2pi$

$=0.0194m$

So, any distance greater than this value will be considered as a long-distance transmission.

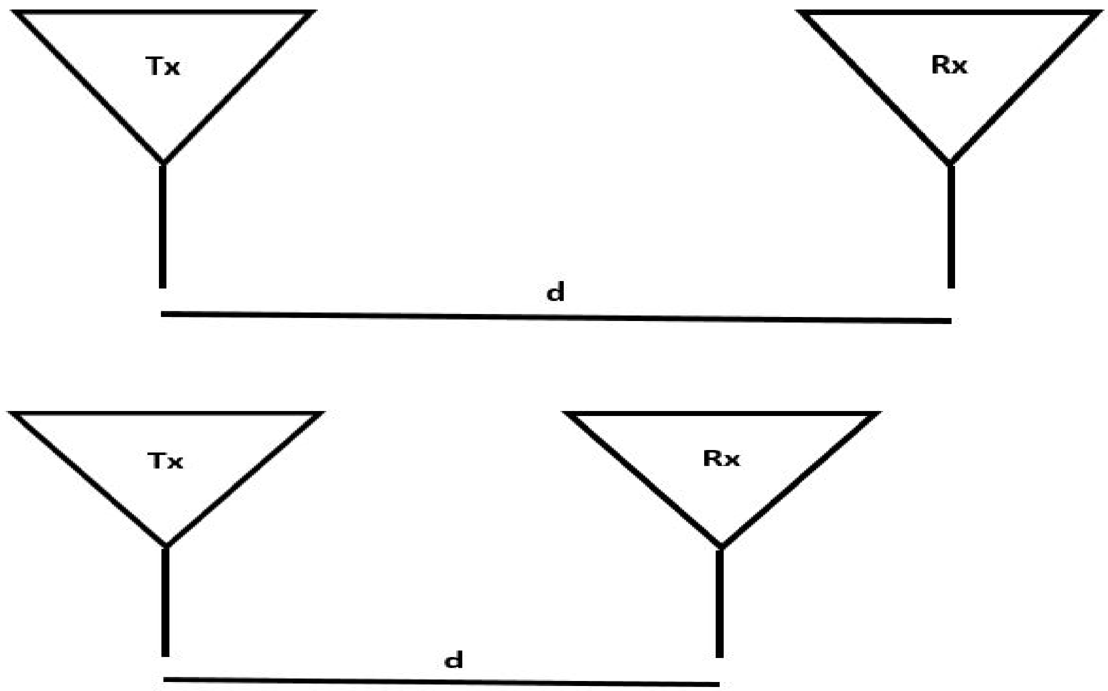

Fig. 4.4 Reducing the distance between antennas

4.2.4 Increasing the transmission frequency

So far, we have seen three methods that can be used, based on the Friis transmission equation, to increase the channel efficiency. From the definition of effective aperture, it can be seen that effective aperture is the ratio of the available power at the terminals of the antenna to the power flux density of a plane wave incident upon the antenna. The effective antenna aperture/area is a theoretical value which is a measure of how effective an antenna is at receiving power. Increasing the aperture can increase the efficiency, however, this also means increasing the physical dimensions of the antenna which in-turn makes it rigid and very hard to change in direction. Therefore, deductions lead to an increase in frequency enhances power transmission over the channel being the good alternative here. Terahertz radiation, also known as sub millimeter radiation, terahertz waves, tremendously high frequency (THF), T-rays, T-waves, T-light, T-lux or THz – consists of electromagnetic waves within the ITU-designated band of frequencies from

0.3 to 3 terahertz (THz). If we use THz range instead of GHz range we can transmit more power because the value of wavelength is decreases with increasing frequency which results more power at the receiving end.

From mathematical analysis it can be deduced that,

Assuming,

$A_r = 0.071521$

$A_t = 0.226168$

If we put different values in the Friis formula of r then we can visualize the changes in the plot. For this case, five different values for r have been considered and the values are as follows

r = 0.25, 0.5, 1, 1.5, 2

t = 1000

λ= 1:0.1:3

$fr \propto \lambda^{(-1)}$

Now from the equation we will have five different values. The equation is as follows

$P = (t^* (Ar * At)) \backslash ((\lambda.^{2}) * (r.^{2}))$

$h = p.^{(-1)}$

Now here let us assume

$Y_1 = h$

From this equation we found the first value for the first value of r. In a similar way we found four more values for four different r values and the values are finally plotte**d for comparison.**

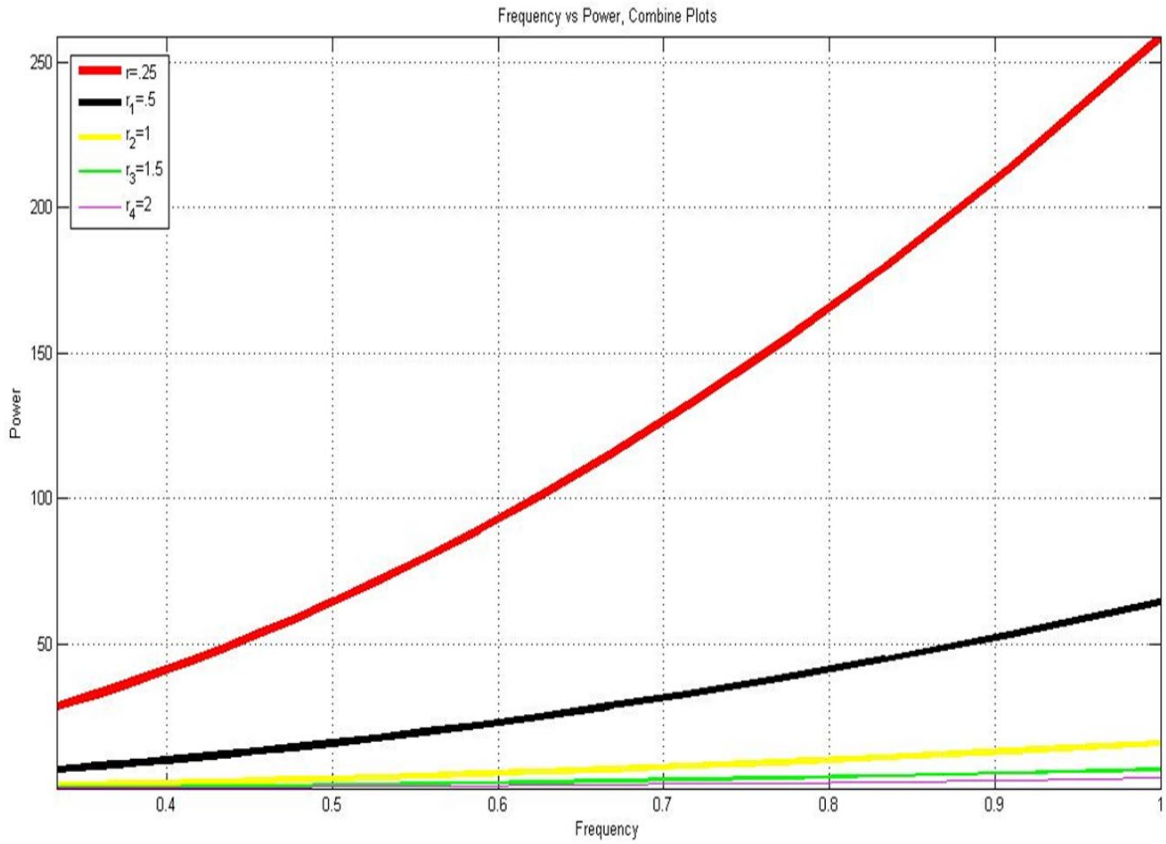

Fig. 4.5 MATLAB simulation for channel efficiency's dependence on the distance between antennas

In the graph there are 5 different curves for different designated values. The curves are marked by red, black, yellow, green and gray colors for easy identification. In the plot, the values of frequency can be manipulated to observe the change is power level.

Computer simulations of the equation for received power were done using MATLAB software. A certain trend in result is exhibited in Fig. 4.5. The figure shows the variable plots for frequency vs power varied at multiple distances. It is evident from the graph that as the value of frequency is increased, the power level rises. The frequency has been varied from 0.4MHz to 1GHz and it was observed that power started to rise from 35mW to 250mW. On the other hand, power level drops as we increase the distance between the two antennas. For better understanding of the scenario the values should be small at the first stages and should be increased sequentially. We have taken very small distance at first and gradually increased the distance and from the graph it can be seen that as the distance increases, power drops drastically. Although shifting frequency from GHz to THz range can improve the transmission efficiency, it has its drawbacks as well. *For example, the new frequency parameter may conflict with any kind of environmental parameter for that reason efficiency may be decreased in some cases.* For the Electromagnetic (EM) waves at THz range, it creates interference with the atmospheric oxygen level. Such interference or conflict absorbs the EM waves into the atmosphere and, hence, affects the transmission efficiency since less of the signal reaches the receiver antenna. The transmission efficiency will drop and, therefore, this imposes a limitation for increasing the frequency up to a certain level.

Chapter 5 Waveforms

5.1 Introduction

For a wireless power system, the signal to be transmitted is a very crucial part since the channel being used is wireless one and its characteristics cannot perfectly be predicted. Therefore, not any arbitrary signal with an arbitrary wavelength can be used. For this reason, we investigate which waveforms can be used to give maximum efficiency at the receiver. Consequently, four types of waveforms are discussed in this chapter, namely; White Noise signa, OFDM signal, One tone signal and finally Chaotic waveform. The criteria used to determine which one is better as done in [3] is PAPR (peak to average power ratio). The role for a high ***PAPR*** in ***WPT*** is to increase diode efficiency in the rectifier circuit of the receiver. More discussion about PAPR is in **5.3.** As it will be shown in the results section, the Chaotic waveform has the highest peak to average power ratio, so it will be the one chosen for this work.

5.2 Mode of operation of a convectional diode

To understand the role of ***PAPR,*** first, the operation of a conventional diode should be understood. For the diode to transmit a forward Bias current fed to it, a certain threshold voltage, V_b, must be surpassed for example 0.7V for a normal silicon diode.

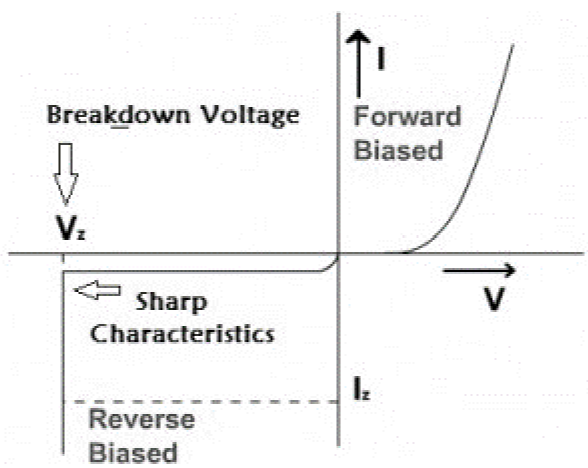

Fig. 5.1 I-V characteristics of a convectional diode

So, if the diode is fed with a voltage which is more than the threshold voltage, a forward bias current will flow. That defines the transmission and absorption of power through a diode.

However, if the diode is in reverse bias mode or if the input voltage is below V_b the power will not be transmitted. Due to the oscillation characteristics of a signal, these diodes cannot keep with the extremely fast transitions of the AC current at GHz frequencies especially if the average power of the signal is below V_b. For this reason, high PAPR is very promising in increasing the efficiency. So, to make the diode on for maximum possible time we had to choose the wavelength in such a way where the PAPR is high and the threshold is met. The role of high PAPR is explained in section 5.4

5.3 Role of PAPR

5.3.1 PAPR meaning

PAPR is defined as the square of the crest factor of a waveform. Crest factor is the amplitude divided by the RMS value of the wavelength. So, we can define the expression of the ratio in dB as

$$PAPR = 10\, log_{10}\left(\frac{max[x^2(t)]}{\langle x^2(t)\rangle}\right) \quad (5.3.7)$$

In the above equation $x(t)$ represents the time domain of the signal of interest whereas $\langle\,\rangle$ represents to the time average operator [3].

The RMS value of the OFDM signal (Fig. 5.2) shown is 0.234 as got from MATLAB. However, this RMS value is less than the V_b of a Schottky which about 0.3V to 0.4V [18]. This means that if this were a one tone signal, the diode would remain off. However, since this signal has a high PAPR, the successive peaks will turn on the diode thus the voltage will be rectified. Therefore, improving the efficiency of the rectifier system. To add on, these peaks come at a very high frequency (GHz range) and this means they will theoretically not give the diode enough time to go off hence further improving the efficiency. That is why high PAPR will make the diode stay on even with lower input power for longer average time. Additionally, if the average input power is high due to the greater number of high peaks the conversion efficiency will be even higher.

5.3.2 PAPR importance

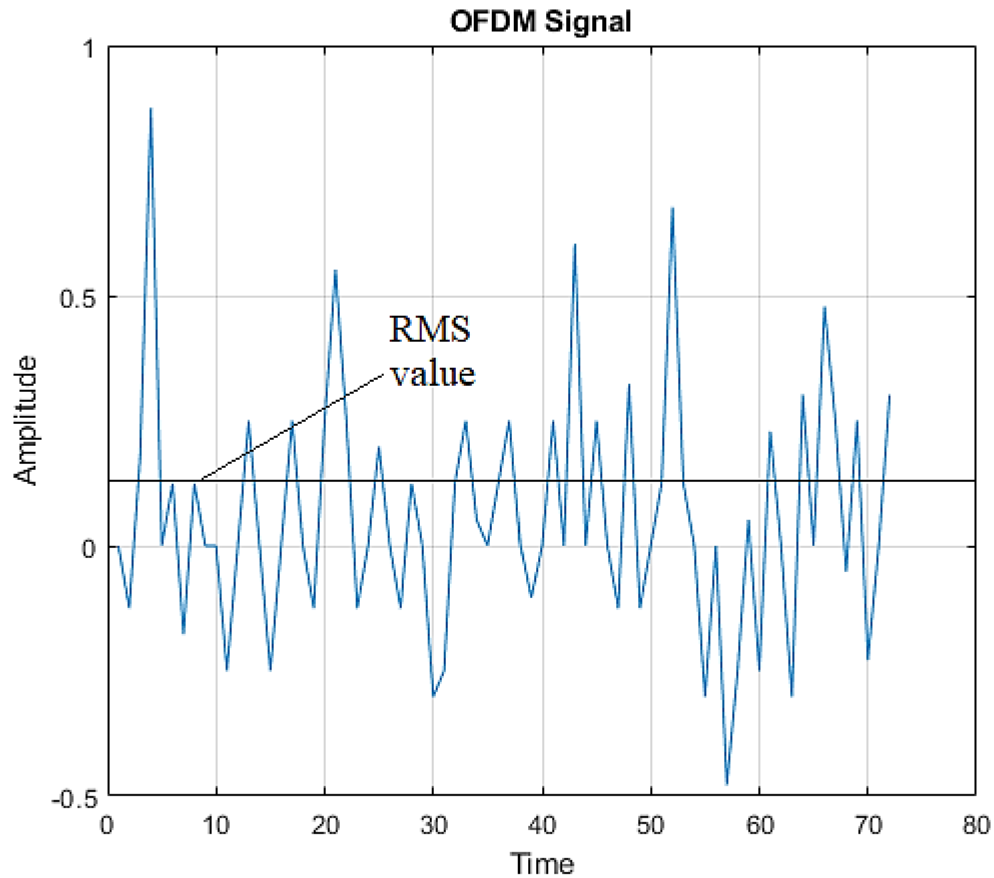

Fig. 5.2 OFDM signal graph from MATLAB simulation results

in comparison to experimented one in [3]. These waveforms are OFDM signals, white noise & chaotic signals and their comparisons are done in section Error! Reference source not found.

5.4 Mathematical comparison of waveforms with high PAPR

As noted in the previous section, OFDM, white noise & chaotic signal are to be compared in this section mainly because all of them have a high peak to average power ratio which is fundamental in improving rectifier efficiency in ***WPT***. A correlation is studied, taking care of the enhancement gotten in the RF-DC efficiency of rectifiers when utilizing these signals in contrast with a one tone signal

5.4.1 One-tone signal

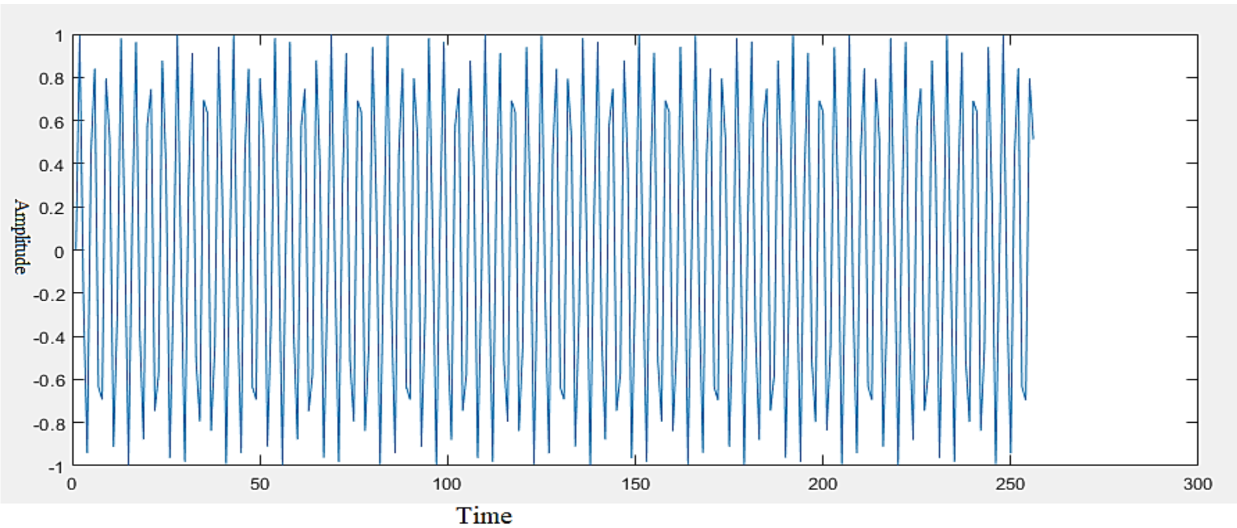

Fig. 5.3 One-tone signal waveform

A single tone signal is shown in the Fig. 5.3. the RMS value is 0.706V and the peak value is 1.0003V. Following the PAPR equation (5.3.1);

$$PAPR = 10log_{10}\left(\frac{1.0003^2}{0.706^2}\right) = 3.027dB$$

5.4.2 Orthogonal Frequency Division Multiplexing

OFDM was introduced in the 1960 while the researchers were trying to minimize the interference between the wireless transmission of two channel of near frequencies [19]. It is a variation of FDM (Frequency Division Multiplexing). FDM is a multiplexing technique used enable transmission of different signals at the same time by subdividing the available bandwidth into non-overlapping (with guard-bands between them) sub-channels in the frequency domain. However, in OFDM there is no guard band between the subcarriers [20]. OFDM signal can cope up with different severe channel conditions like high attenuation high frequencies in a long copper wire, narrowband interference and frequency-selective fading due to multipath without complex equalization filters. Due to these multi-carrier aggression schemes, OFDM signal presents high PAPR. Depending on the number of used sub-carriers (N), the maximum theoretical PAPR of an OFDM signal can equal N, as long as all the sub-carriers add up in phase. However, as the sub-carriers of the OFDM signal are not modulated equally, the in-phase condition is not reached which prevents obtaining the maximum theoretical PAPR. Fig. 5.2 above shows the OFDM signal graph got from MATLAB simulation.

From equation (5.3.1), if we insert the RMS value and maximum value of the graph in Fig. 5.2 as got in MATLAB, we get;

$x = 0.234\text{V}$

And

$max(x) = 0.422\text{V}$

Therefore,

$$PAPR = 10log_{10}\left(\frac{0.422^2}{0.234^2}\right) = 5.12dB$$

5.4.3 White noise signal

White noise is the type of noise available at all frequencies. That is to say, it has an infinite bandwidth. In practical, researchers generate band-limited signals with near approximate white noise characteristics. Fig. 5.4 below shows the white noise signal generated in MATLAB.

The RMS value of the white noise signal is 2.013 and its maximum value is 6.127.

Feeding the above values in equation (5.3.1), we get;

$$PAPR = 10log_{10}\left(\frac{2.1425^2}{0.9022^2}\right) = 7.512dB$$

Evidently, the white noise signal has a higher PAPR value than the OFDM signal which is the same result got from experiments performed in [3].

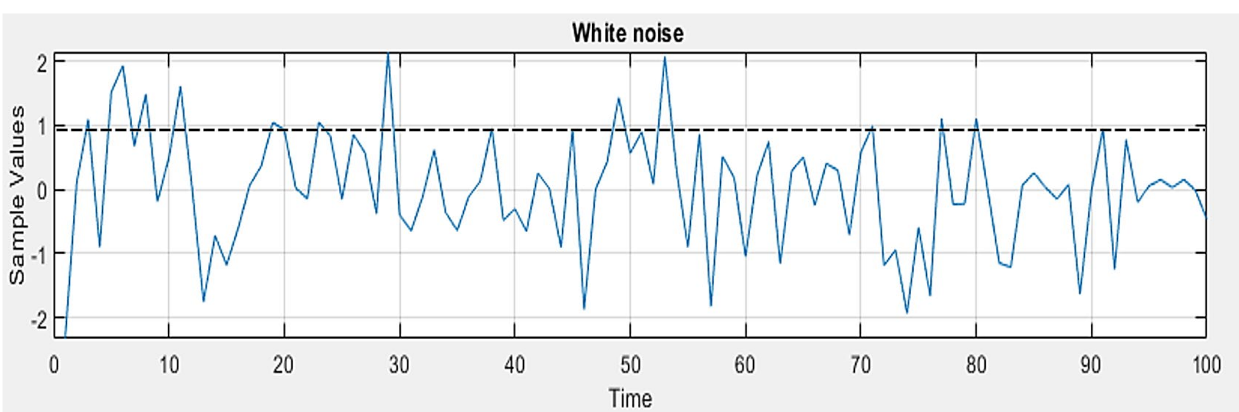

Fig. 5.4 White Noise Signal generated in MATLAB

5.4.4 Chaotic Waveforms

Following quite a while of research, chaotic remains a quickly developing part of science and engineering where an immense amount of scope to improve and there are lot to understand. What is still very difficult is determining some of the characteristics of chaos. A chaotic signal is a continuous-valued signal with positive, finite entropy rate and infinite redundancy rate. A chaotic signal which sometimes called nonlinear signals is characterized by its high sensitivity to the parameter and initial condition perturbations, the random-like nature, and broadband spectrum. This chaos is widely used in physics, chemistry, biology, acoustics, engineering, wireless technologies, sonar systems and networks, fiber optic systems, even the encryption of data too. Because many communications and ranging systems operate at microwave frequencies, a chaotic signal generator in this regime is of considerable interest. Although there are many classical electrical circuits that can produce broadband chaotic waveforms, it is often difficult to scale these systems to the microwave regime because in high-speed systems, the time delay associated with signal propagation cannot easily be ignored in comparison to the dynamical timescales. Chaotic generators that expressly rely on time-delayed feedback can take advantage of these unavoidable signal propagation delays [21]. A chaotic signal is shown in Fig. 5.5.

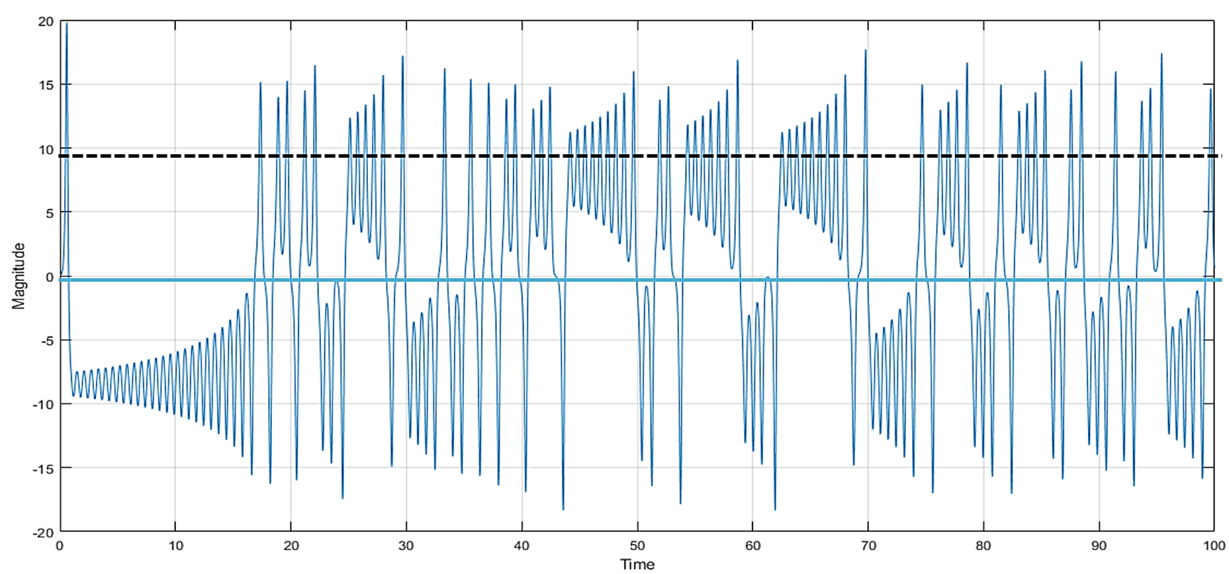

Fig. 5.5 Chaotic Signal waveform generated in MATLAB

Values attained from the simulation results give the RMS value of the signal as 1.7239V and the peak value as 3.3636V.

According to equation (5.3.1) the value for PAPR;

$$PAPR = 10log_{10}\left(\frac{19.8185^2}{8.0205^2}\right) = 7.857dB$$

As expected the PAPR value of the chaotic waveform is greater than those of both one-tone signal and OFDM signal and slightly also greater higher than that of the white signal. Hence being in agreement with results attained experimentally in [3]. It can also be seen that the chaotic signal has more peaks above the rms value when compared to the white noise hence this is beneficial for the rectification

Results and conclusion

Signal Type	RMS value (V)	Peak Value (V)	PAPR (dB)
One-tone	0.706	1.0003	3.027
OFDM	0.234	0.422	5.12
White Noise	0.9022	2.1425	7.512
Chaotic	8.0205	19.8185	7.857

Table 1: PAPR comparison for different signals

The results shown in the table above justify the argument for Chaotic waveforms being better than White Noise, OFDM and One-tone signal by having a higher PARP value. Nevertheless, the argument for chaotic waveforms being promising better efficiency are practically valid as experimented values in [3] also come give the same conclusion. This result brings up an interesting observation and that is PAPR is not the ultimate test in proving which signal would give better efficiency since one signal may have a higher peak value due to one single very high peak. In contrast, this may not be comparable to another signal with a higher average number of peaks which are a bit lower than the first signal’s single peak value.

Chapter 6 Rectenna

6.1 Introduction

The rectenna (*receiving antenna*) is one of the most integral devices used for Wireless Power Transmission via radio waves, microwaves or for energy harvesting. In MPT, the rectenna is a key component which is used to receive and convert microwave power to DC power. It is a passive element with rectifying diodes that operates without an internal power source [11]. A general block diagram of a conventional rectenna is shown in Fig. 6.1. The input power is fed into the rectenna system through a receiving antenna which then passes the power through a low pass filter circuit after which the filtered signal is rectified into DC power and fed into a resistive load after being passed through an output filter. The rectenna has many desirable characteristics which includes maximum receiving of input power through the antenna, optimum rectification in the rectifier circuit and the rectenna must be suitable for a wide bandwidth of frequencies. Various types of antenna and rectifier circuits can be used depending on the system's requirement and the users' demands.

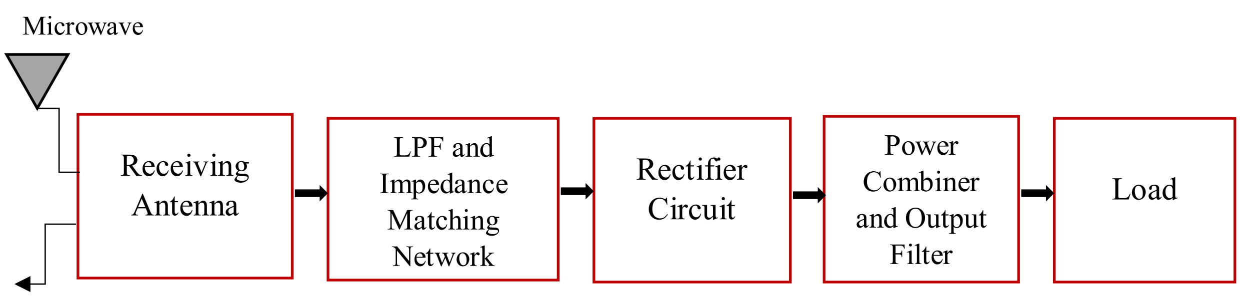

Fig. 6.1 Block diagram of receiving end of the MWPT System (Rectenna)

6.2 Significance of Rectenna Array

The efficiency of the rectenna greatly depends on the amount of power received by the antennas. In general, a single rectenna cannot provide sufficient power for device operation. Thus, the rectenna is split into partitions or arrays, where the antennas can, theoretically, absorb 100% of input microwaves [22]. A general diagram of the rectenna array with uniform division of panels is shown in Figure 2. In case of narrow beam transmission of microwave, this configuration offers the most efficient power transmission scheme. The receiving antenna panel is divided into N divisions, where, greater the power division greater is the system efficiency [12]. The input power at each antenna is rectified individually to separately harvest DC power which can then be combined using a DC combiner before being fed into a load. This configuration is suitable for large rectenna arrays.

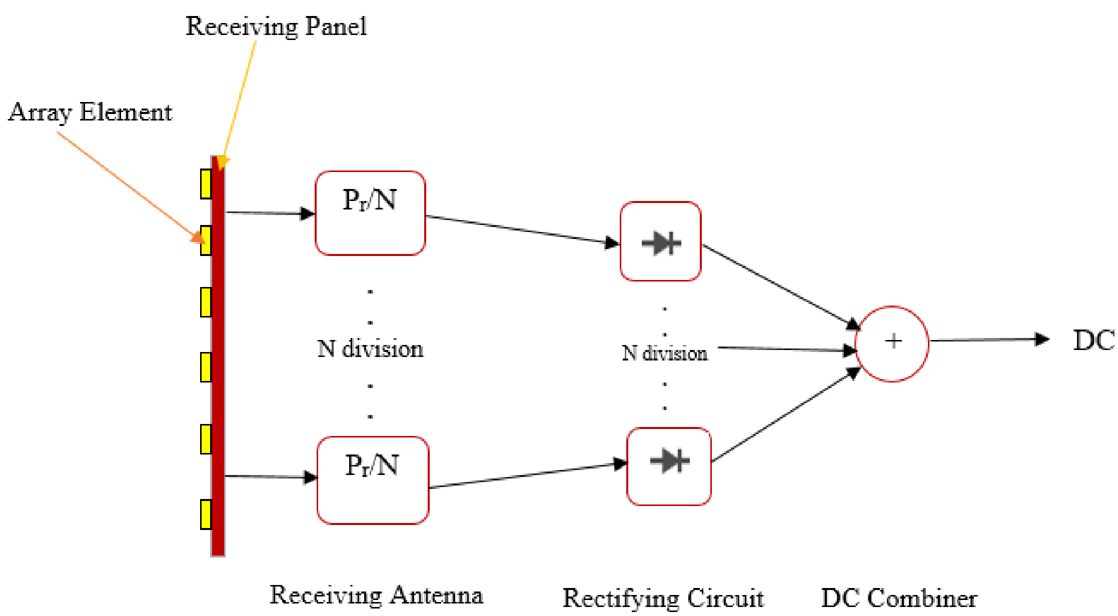

Fig. 6.2 Uniform Division of Panel in a Rectenna Array

Furthermore, using an antenna array limits the amount of input power transmitted into the diodes of the rectifier circuit. This is an important factor since the diodes, traditionally used for RF-DC conversion, gives optimum output at low input voltage, which is discussed in Section 6.7.

Moreover, working frequency is also an important factor which is to be considered while designing a rectenna since at low frequencies high gain antennas tend to be quite large. Whereas, increasing the frequency allows the use of more compact antennas.

6.3 Importance of Impedance Matching

In microwave circuits, impedance matching is a very significant concept since it helps to maximize the power transfer from the source to the load or minimizes the signal reflection from the load. Any discontinuity in the characteristic impedance of the circuit, at any part, leads to some of the incident power to be reflected back to the source as it reaches the point in question.

If V_0^+ is the amplitude of the incident voltage, in the positive Z direction, as shown in Fig. 6.3 and V_0^- is the reflected voltage's amplitude, then the reflection co-efficient, Γ, is given by

$$\Gamma = \frac{V_0^-}{V_0^+} \tag{6.3.8}$$

Now, in terms of impedance,

$$\Gamma = \frac{Z_l - Z_0}{Z_l + Z_0} \tag{6.3.9}$$

Where, Z_l is the load impedance and Z_0 is the characteristic impedance of the transmission line.

Therefore, the Return loss, RL, which represents the amount of power reflected back to the source, is given by,

$$RL = -10log_{10}(|\Gamma|^2) = -20log_{10}(|\Gamma|)\ dB$$

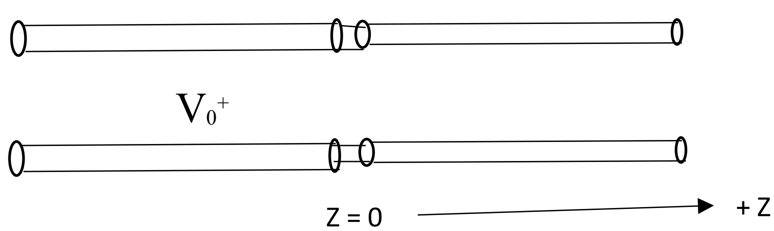

Fig. 6.3 Two wire microwave transmission line

Hence, for all the po [illegible] to be equal to the characteristic impedance of the transmission line which is termed as impedance matching thereby making the value of the RL be infinite, meaning no power is reflected.

Rectifiers, usually, use non-linear elements such as diodes or transistors for impedance matching, however, the input impedance varies with frequency, input power and load impedance which is a challenge yet to be tackled [23].

6.4 Basics of Rectifier

A rectifier is a circuit which converts the microwave input signal, received by the antenna, into a zero frequency DC signal. In combination with some passive components, high frequency diodes are the heart of the rectifier circuit. The basic function of a rectifier, in both time and frequency domain, is shown below.

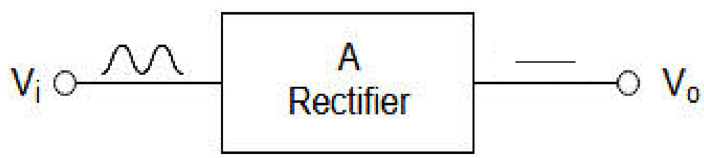

Fig. 6.4 General Block Diagram of a Rectifier

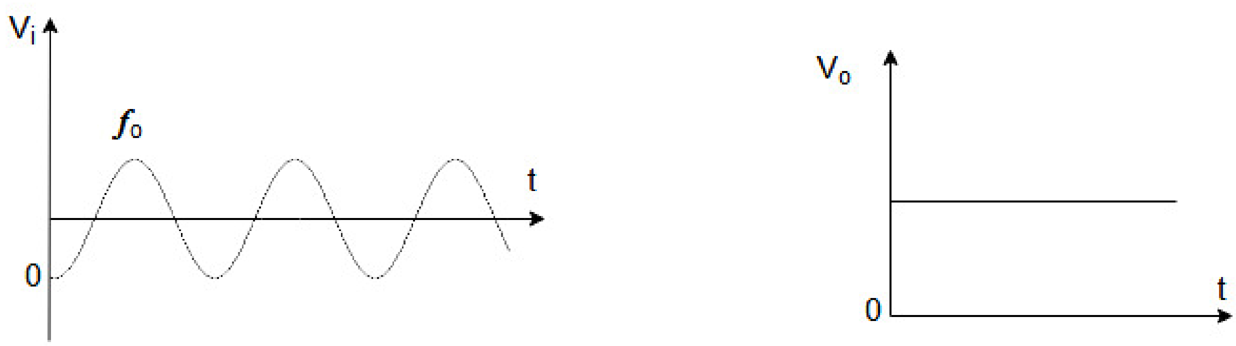

Fig. 6.5 Time Domain representation of a signal before and after Rectification

In time domain, the graphs show a high frequency, f_o, microwave signal being rectified into a zero frequency DC signal.

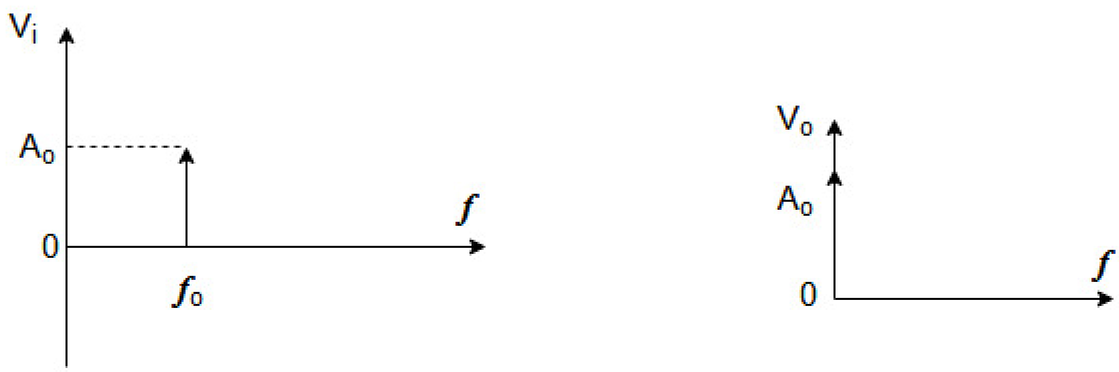

Fig. 6.6 Frequency Domain representation of a Signal before and after Rectification

The frequency domain graphs represent how a fixed frequency, f_o, microwave or an AC signal is converted into a zero frequency DC signal with the same amplitude.

The efficiency of a rectifier mainly depends on the voltage sensitivity of the diode and also the overall efficiency of the diodes. Thus, the selection of a suitable diode is extremely crucial for high efficiency rectification.

6.5 Single-shunt Rectifier

Initially, in MPT, a single- shunt full wave rectifier was used which consists of a diode and capacitor connected in parallel along with a $\lambda_g/4$ transmission line, where, λ_g is the effective wavelength of the input microwave. Fig. 6.7 shows the block diagram of a rectenna with a single-shunt rectifier. This rectifier can, theoretically, rectify the microwave with 100% efficiency since it consists of only one diode [11]. The antenna at the receiving end absorbs the high frequency microwave which then passes through a low pass filter where higher harmonics are cut off. The low frequency input goes through a full wave rectification, where the diode converts the bi-directional AC signal into a unidirectional DC signal which means the negative cycle is converted into positive cycle. After passing through the long transmission line, the full wave signal is converted to DC by the capacitor. The capacitor helps in further rectification by reducing the ripple voltage of the unidirectional DC signal. Before being fed into a load, the signal might be passed through a DC/DC or DC/AC converter as per the requirement.

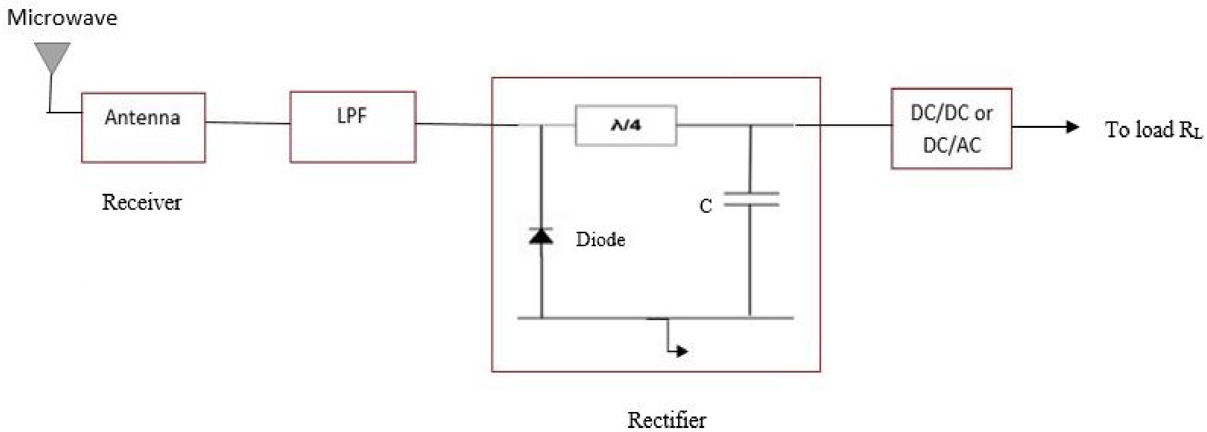

Fig. 6.7 . Block Diagram of a rectenna with a single-shunt full wave rectifier

An input impedance exists in the diode of the diode which is given by the following equations [11]:

$$Z_L = \frac{R_L}{1 + j\omega C R_L}$$

$$Z_{in} = \frac{Z_L + jZ_0 \tan(\beta l)}{Z_0 + jZ_L \tan(\beta l)} Z_0 \qquad (6.5.10)$$

$$\beta = \frac{2\pi}{\lambda_g}$$

Where, R_L is the load resistance, C is the capacitance of the output filter, Z_0 is the characteristic impedance of the distributed line and its circuit, l is the length of the distributed line, β is a phase constant and ω is the angular frequency of the input electromagnetic wave.

6.6 Class-F Rectifier

The class-F rectifier is very similar to the single-shunt rectifier with some small improvements. The single-shunt diode class-F rectifier comprises of an ideal DC block, ideal RF choke, a diode, a lossless transmission line and a source impedance which is set to be conjugate match to the rectifier input impedance at various input power levels. An ideal class F rectifier circuit topology is illustrated in Fig. 6.8 [24]. The DC block capacitor acts as an open circuit to filter away any DC component, which might be present or created, to avoid interference with the input microwave signal. Then, a RF choke circuit is used which acts as a low pass filter that 'chokes' out higher frequencies and allows lower ones to pass through. A choke is a further modification of an inductor which helps to filter out signals. It is made up of a coil of insulated wires wound on a magnetic core. The choke's impedance increases with an increase in frequency which is how it is able to block high frequency signals while letting low frequency ones to pass through. The class F rectifier has a harmonic termination network, in contrast with the single-shunt rectifier, which cuts off the diode's higher harmonics. Theoretically, it presents the diode with zero impedance at even harmonics and with infinite impedance at odd harmonics. The harmonic transmission network consists of transmission lines of three different lengths, $\lambda/12$, $\lambda/8$ and $\lambda/4$ [24] where the lengths are pre-determined to give out the required impedance. These lengths can be varied for a better impedance matching. These overall impedances terminate the diode's higher harmonics signals. Finally, the rectifier circuit uses a Schottky diode for optimum output. It is conventional to use just one diode in the rectifier circuits to minimize the diode loss.

In comparison with the single-shunt rectifier, the class-F rectifier is a better choice since it consists of an additional RF choke circuit to remove higher harmonics and, also, it has an upgraded impedance matching network. This harmonic termination network is a replacement of the capacitor in the single-shunt rectifier circuit since the capacitor is insufficient to control the higher harmonics.

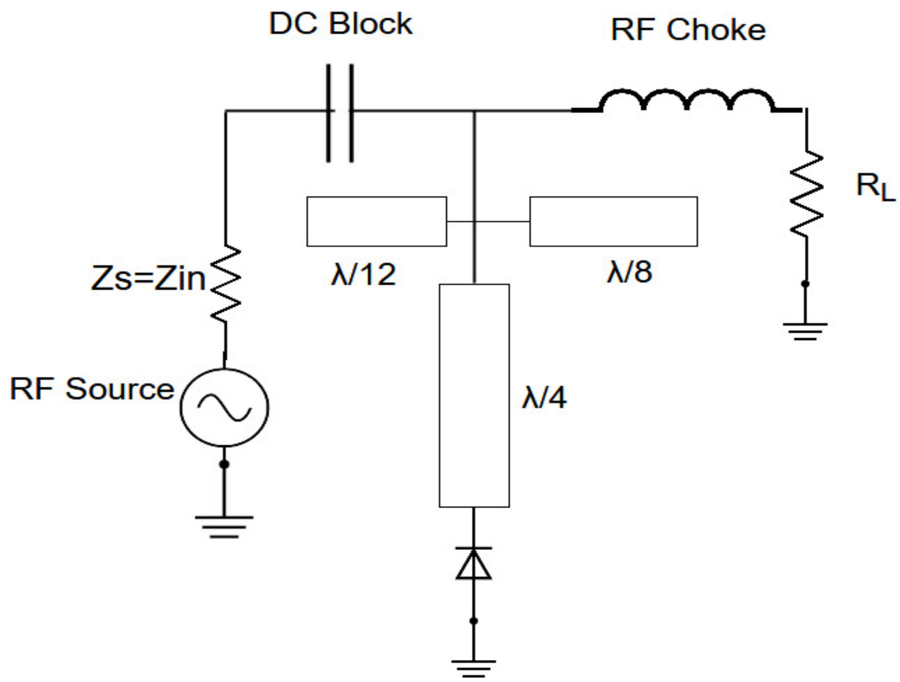

Fig. 6.8 Ideal Class-F Rectifier

6.7 Basics Principle of the Schottky Diode

Unlike the traditionally used Si diode which is a pn-junction between two semiconductor materials, Schottky diode is a metal-semiconductor junction, either p or n, where electrons flow from the semiconductor material to the metal and fill up the energy states in the metal. This flow of electrons forms the depletion region across the junction and the difference in energy levels between the metal and the semiconductor is known as the Schottky barrier. Fig. 6.9 [25] shows the diode I-V characteristics difference between a Si diode and a Schottky diode. From the figure it can be observed that unlike the commonly used Si diode, Schottky diode turns on at a much lower voltage. The threshold voltage of a Schottky diode is 0.3V which is much lesser than a Si diode and, this is the reason why Schottky diodes are preferable when it comes to low input power operation. The diode turns on at a very low input power without requiring much threshold power loss. Moreover, in contrast to the conventional p-n junction diode, current in the Schottky diode is only carried by majority carriers, which are the electrons in a n-doped semiconductor, since no minority carrier, which are holes in a n-doped semiconductor, charge storage effects are present. One disadvantage of Schottky diode is that, along with having a lower threshold voltage, it also has a lower breakdown voltage. This means that it is not quite suitable to use for high input power.

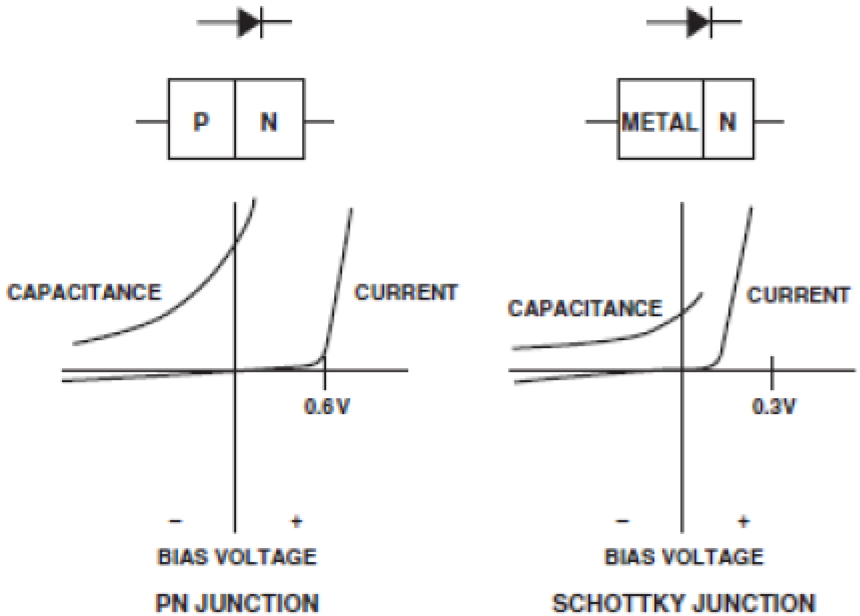

Fig. 6.9 I-V characteristics of pn junction and Schottky junction diodes

6.8 Diode Efficiency

The RF-DC microwave conversion efficiency of a rectifier is simply a ratio of the rectified output DC power and the RF incident power which is as follows:

$$\eta = \frac{DC\ output\ power}{RF\ input\ power} = \frac{P_{DC}}{P_{RF}}$$

The rectifier conversion efficiency is determined by some factors which includes diode loss, loss due to impedance mismatch, and substrate and conductor losses in printed circuit board (PCB). Amongst these, diode loss is the most dominant one [24].

Diodes show different trend in efficiency for low and high input power levels. In the low input power region, diode loss occurs because of forward diode built-in potential which is denoted as V_{bi} whereas, in the high input power region, the loss occurs due to diode breakdown voltage, V_{br}. In this section, our main focus is on the low input power region where the diode loss [24] is given by,

$$Diode\ Loss = \frac{V_{bi}}{V_o + V_{bi}}$$

Where, V_o is the diode reverse bias voltage.

On a different note, in the high input power region the reverse peak voltage across the diode exceeds the diode breakdown voltage which causes a huge amount of current to flow through the diode causing a significant loss in the DC output power which results in a huge drop in the rectification efficiency. The general trend in change in efficiency in both low and high input powers is illustrated in Fig. 6.10 [24]. It shows how the efficiency increases at low power input until a diode reaches breakdown voltage after which the efficiency falls drastically due to the flow of huge amount of current.

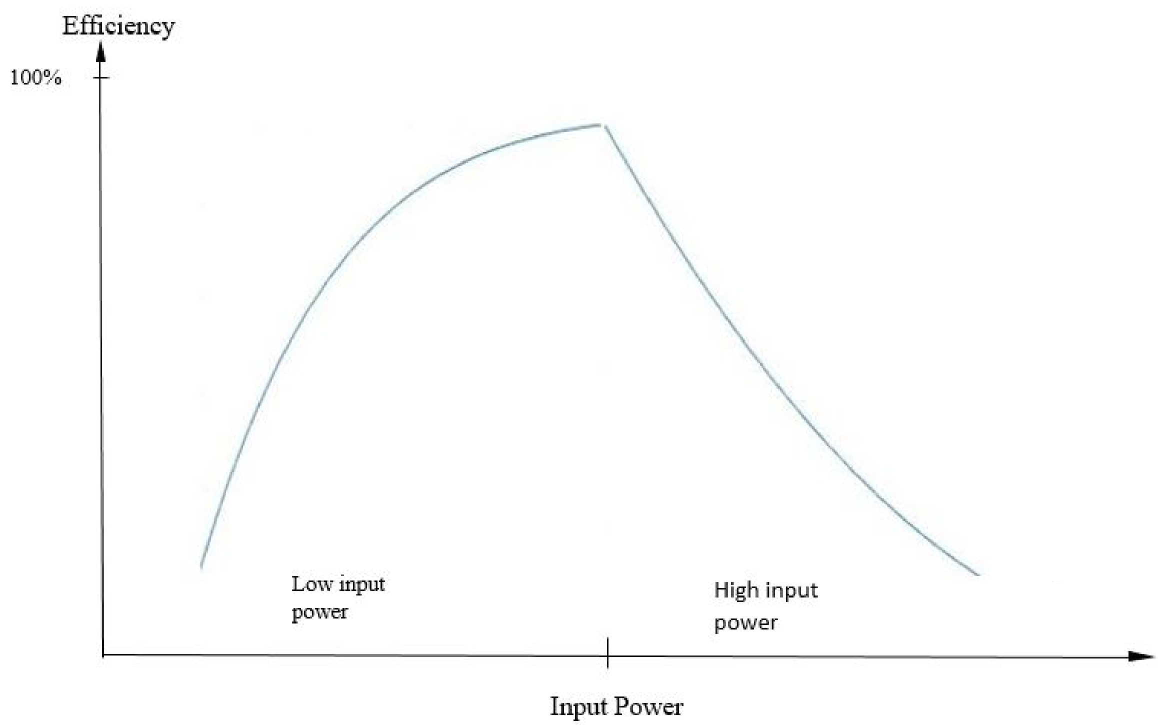

Fig. 6.10 General microwave rectifier conversion efficiency at low and high input power levels

This paper consists of a thorough study of the diode equivalent circuit shown in Fig. 6.11 [24]. The internal circuit of a diode comprises of a series resistor, R_S, a non-liner junction resistor, R_j, and a non-linear junction capacitor, C_j. The diode efficiency analysis assumes an ideal class-F termination network up to infinite harmonics.

From the dashed line of the Fig. 6.11, it can be seen that the load resistor, R_L has the same DC voltage and the opposite DC current as that of the diode. Thus, the load resistance and the output power are defined as,

$$R_L = -\frac{V_o}{I_o} = \frac{-2I_P R_S - \pi V_{bi} + \pi V_P}{2I_P} \tag{6.8.11}$$

$$P_{OUT} = -V_o I_o = \frac{I_P(-2I_P R_S - \pi V_{bi} + \pi V_P)}{2\pi^2}$$

The efficiency of the diode is thus derived as,

$$\eta = \frac{P_{OUT}}{P_{IN}} = \frac{I_P(-2I_P R_S - \pi V_{bi} + \pi V_P)}{2\pi^2 P_{IN}} \tag{6.8.12}$$

The diode loss is mainly introduced by the diode parameters C_j, R_S and V_{bi}. The losses due to these parameters are defined as follows,

$$P_{Loss,R_S,V_{bi}} = \frac{I_P(I_P \pi R_S + 4V_{bi})}{4\pi}$$

$$P_{Loss,C_j} = \frac{4f^2 C_j^2 V_P^2 R_S}{\alpha}$$

Now, since the total input power is the summation of the total output power and the total power loss, another equation for diode efficiency has been derived as,

$$\eta = \frac{P_{OUT}}{P_{IN}}$$

$$= \frac{P_{OUT}}{P_{OUT} + P_{LOSS,C_j} + P_{LOSS,R_S,V_{bi}}}$$

$$\eta = \frac{2I_P(-2I_PR_S-\pi V_{bi}+\pi V_P)}{2I_P(-2I_PR_S-\pi V_{bi}+\pi V_P)+\pi I_P(I_P\pi R_S+4V_{bi})+\frac{16\pi^2 f^2 C_j^2 V_P^2 R_S}{\alpha}} \tag{6.8.13}$$

Where,

I_P = peak inverse voltage

V_P = peak voltage

V_{bi} = forward diode built-in potential

f = frequency

By solving equations (6.8.11), (6.8.12) and (6.8.13), the diode conversion efficiency can be calculated. C_{jo}, R_S and V_{bi} are the diode parameters which are provided by the manufacturer and the value of α is assumed to be 0.1. The remaining parameters P_{IN}, f and R_L are to be selected by the designer as per the requirements. In this paper first P_{IN} is varied keeping f and R_L constant at 900MHz and 510Ω respectively to analyze the effect of increasing input power on the diode efficiency. Secondly, the frequency has been varied by keeping P_{IN} and R_L constant at 20mW and 510Ω respectively to analyze the effect on diode efficiency.

Since the efficiency of a rectifier circuit mainly relies on the diode, the selection of a suitable diode for the rectifier is extremely crucial. Traditionally, Schottky diodes are used in the RF-DC rectifier circuits instead of the commonly used Si diodes.

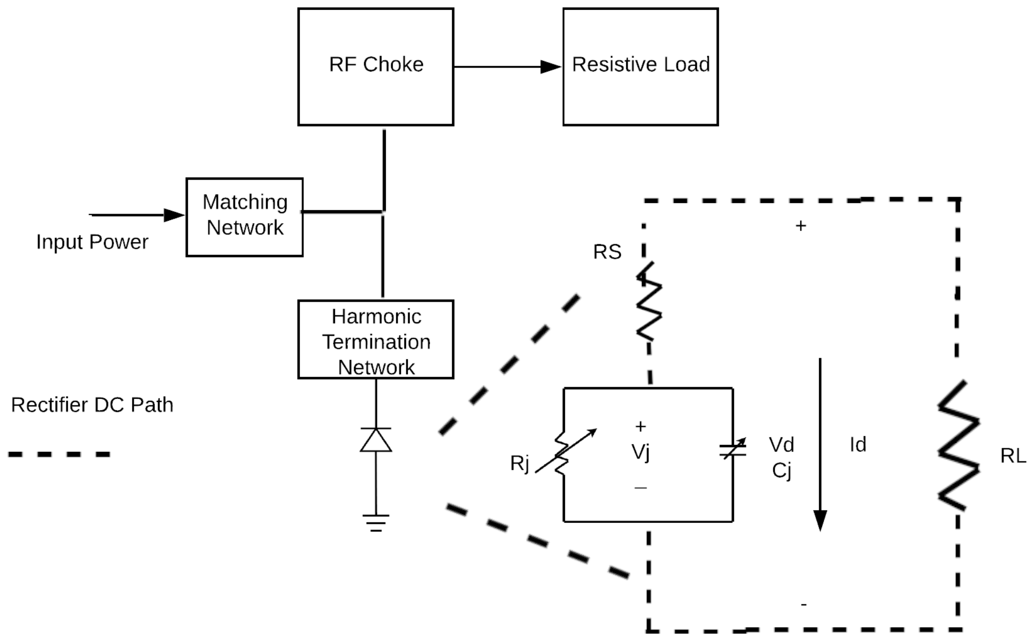

Fig. 6.11 Circuit Topology of Class-F rectifier and internal circuit of diode

In addition to single-shunt and class-F rectifiers there are other types of rectifiers as well for RF-DC rectification which include class-B, class-C, class-D class-E and a few others. Commonly, class-F is used for rectification since it has the most conversion efficiency and minimum power loss. Some recent researchers have also used the inverse class-F rectifier, the work of which is still in progress. The rectifiers, mentioned, mainly differ in the way the circuit components are arranged, and this plays a major role in the conversion efficiency. For example, class-C rectifier has a resonator circuit incorporated in the rectifier circuit which cuts off higher harmonics. However, this extra circuit components possess some power loss due to which efficiency decreases. On the other hand, class-D rectifier uses two diodes for rectification which adds up to the diode loss.

6.9 Mathematical Modelling of Diode Efficiency with Simulation Results

6.9.1 Low Power vs Efficiency Comparison

The following are the diode parameters which has been specified by the manufacturer:

		Diode Models				
Parameters	**Units**	**HSMS-282x**	**HSMS-285x**	**HSMS-286x**	**SMS-7621**	**SMS-7630**
C_{jo}	pF	0.70	0.18	0.18	0.10	0.14
R_S	Ω	6	25	6	12	20
V_{bi}	V	0.65	0.35	0.65	0.51	0.34

Table 2 Diode parameters specified by manufacturer

The efficiency has been calculated for microwave at 900MHz. The value for load resistance and α has been assumed [24].

Fixed Parameters:

Parameters	**Units**	**Values**
F	MHz	900
R_L	Ω	510
α	-	0.1

Table 3: Fixed parameters

For each of the diodes, the input power, P_{IN}, has been varied and the corresponding efficiency, η, has been calculated. The data are as follows:

P_{IN} (mW)	**Efficiency, η (%)**				
	HSMS-282x	**HSMS-285x**	**HSMS-286x**	**SMS-7621**	**SMS-7630**
10	59.2	72.9	72.2	75.3	76.8
15	63.0	74.9	76.0	78.3	78.9
20	65.2	76.2	78.4	80.2	80.2
25	66.8	77.0	80.1	81.6	81.1
30	68.0	77.7	81.3	82.5	81.7

Table 4: Efficiency results from mathematical analysis

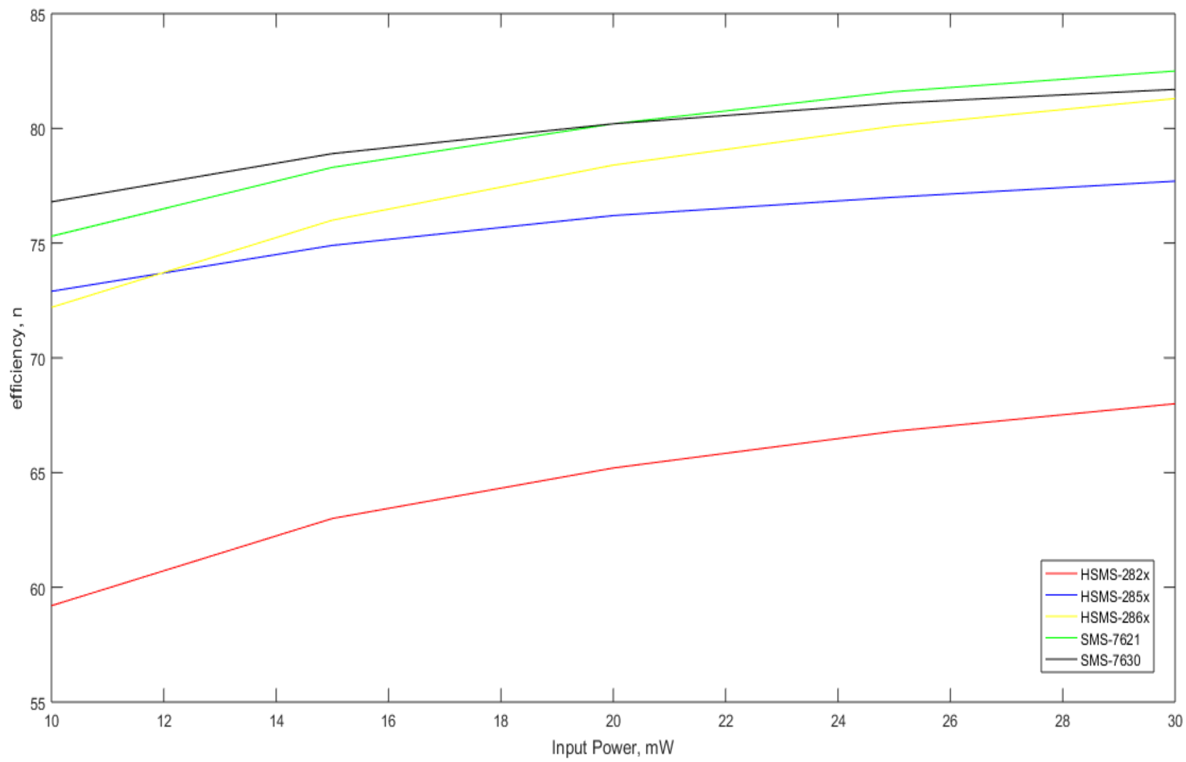

Fig. 6.12 Calculated efficiency of multiple diode models for different low input power

Fig. 6.12. illustrates the change in diode efficiency with an increase in input power level. The input power has been limited to 30mW since beyond this, the diodes cross their breakdown voltage and the efficiency drops drastically as huge amount of current flows through the diodes. For different diodes, the input power level at which breakdown occurs will vary slightly and, thus, 30mW is an approximate value since none of the diodes used goes to breakdown beyond this [24]. The main aim was to find out the trend in change in efficiency as the input power is varied. From the plot, it can be seen that the diode efficiency increases as we increase the input power level as long as the diode does not reach breakdown. From the graph in Fig. 6.12 Calculated efficiency of multiple diode models for different low input power, it can be concluded that HSMS-286x, SMS-7621and SMS-7630 are the most suitable diodes since they have very high efficiency values. However, other factors, such as effects of frequency of input signal, load resistance, to mention but a few, have to be considered as well before drawing a final conclusion regarding which is the most suitable diode for optimum rectification. This comparison analysis provides an aid in picking the best diode for the rectifier circuit.

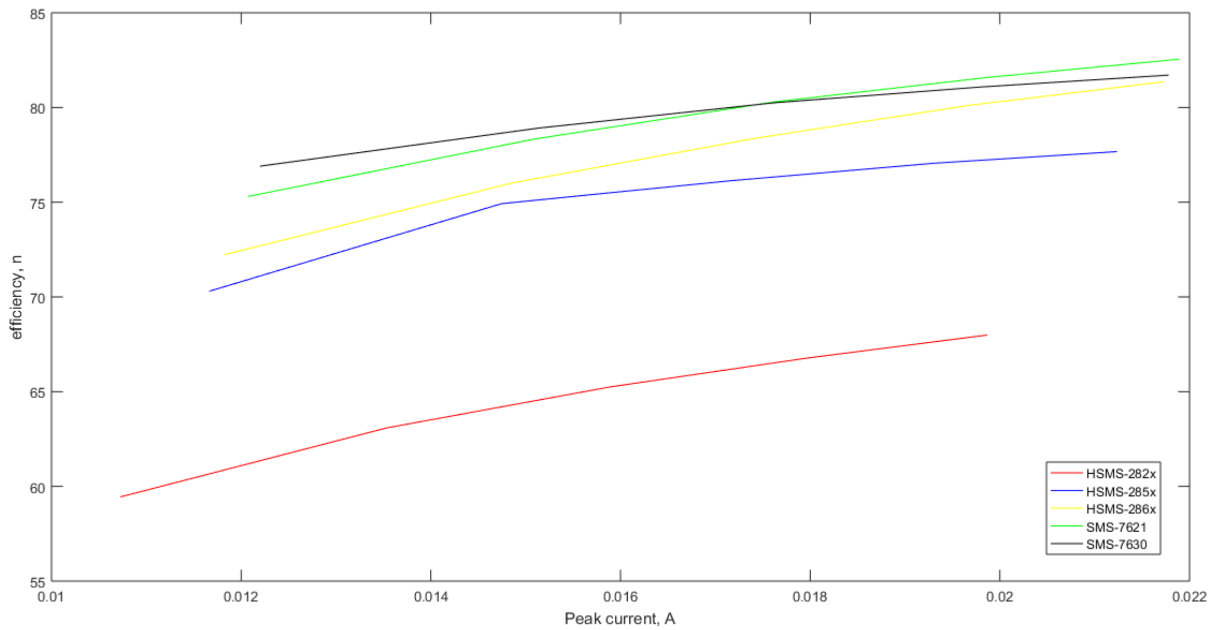

Fig. 6.13 Simulation results of diode efficiency with increasing inverse peak current

Fig. 6.13 helps to validate the calculated values of diode efficiency with increasing input power. Notice, the increase in the peak voltage of diode increases the diode's conversion efficiency the same way as input power does, the efficiency has an increasing trend, since the input power is proportional to the peak current. From the calculations we can deduce this relation between the peak current and input power, with increasing input power the peak current increases. Therefore, Fig. 6.12 and Fig. 6.13 combined confirms that the diode conversion efficiency increases with increasing input power level until the diode reaches its breakdown.

6.9.2 Mathematical validation

The following is the extensive efficiency calculation for a diode with the given parameters at an input power of 10mW.

<u>Diode Model: HSMS-286x</u>

C_{jo} = 0.18pf

R_S = 6Ω

V_{bi} = 0.65V

f = 900MHz

R_L = 510Ω

α = 0.1

Starting with,

$$R_L = \frac{-2I_P R_S - \pi V_{bi} + \pi V_P}{2I_P}$$

=> $510 = \frac{-12*I_P - 0.65*\pi + \pi * V_P}{2*I_P}$

$$V_P = \frac{1032}{\pi} I_P + 0.65 \quad (6.9.14)$$

$$\eta = \frac{I_P(-2I_P R_S - \pi V_{bi} + \pi V_P)}{2\pi^2 P_{IN}}$$

$$= \frac{I_P(-12I_P - 0.65\pi + \pi V_P)}{2\pi^2(10 \times 10^{-3})} \quad (6.9.15)$$

Substituting equation (6.9.14) into equation (6.9.15) we get,

$$\eta = \frac{1020 * I_P^2}{0.02 * \pi^2} \quad (6.9.16)$$

From equation (6.8.13),

$$\eta = \frac{2I_P(-2I_P R_S - \pi V_{bi} + \pi V_P)}{2I_P(-2I_P R_S - \pi V_{bi} + \pi V_P) + \pi I_P(I_P \pi R_S + 4V_{bi}) + \frac{16\pi^2 f^2 C_j^2 V_P^2 R_S}{\alpha}}$$

(6.9.17)

$$\frac{16\pi^2 f^2 C_j^2 V_P^2 R_S}{\alpha} = \frac{16\pi^2(900\times10^6)^2(0.18\times10^{-12})^2 V_P^2\times6}{0.1}$$

$$= (2.4866 \times 10^{-4})V_P^2 \tag{6.9.18}$$

Substituting equation (6.9.14) into equation (6.9.18) we get,

$$(2.4866 \times 10^{-4})V_P^2 = 2.4866 \times 10^{-4}\left(\frac{1032}{\pi} I_P + 0.65\right)^2 \tag{6.9.19}$$

Now substituting equation (6.9.19) into equation (6.8.13) we get,

$$\eta = \frac{2 * I_P(-12 * I_P - 0.65\pi + \pi * V_P)}{2 * I_P(-12 * I_P - 0.65\pi + \pi * V_P) + \pi * I_P(6\pi I_P + 2.6) + 2.4866 * 10^{-4} * (\frac{1032}{\pi} I_P + 0.65)^2}$$

$$= \frac{2040 I_P^2)}{(2126.051)I_P^2 + (8.274)I_P + (10^{-4})} \tag{6.9.20}$$

Now, substituting equation (6.9.16)into equation (6.9.20) we get,

$$(2126.051)I_P^2 + (8.274)I_P - 0.395 = 0$$

Solving this we get,

I_P = 0.01182 A

Substituting this value into equation (6.9.16) gives us,

η = 0.722 = 72.2%

The same calculations have been carried out for different input power values to obtain the respective efficiencies for different diode models.

6.9.3 Frequency vs Efficiency Comparison

The following are the diode parameters which has been specified by the manufacturer:

		Diode Models				
Parameters	**Units**	**HSMS-282x**	**HSMS-285x**	**HSMS-286x**	**SMS-7621**	**SMS-7630**
C_{jo}	pF	0.70	0.18	0.18	0.10	0.14
R_S	Ω	6	25	6	12	20
V_{bi}	V	0.65	0.35	0.65	0.51	0.34

Table 5: Parameters specified by manufacture

The efficiency has been calculated for microwave at a low input power of 20mW since at this power level, approximately, most of the diodes used have the optimum efficiencies [24]. The values for load resistance and α have been assumed.

Fixed Parameters:

Parameters	Units	Values
P_{IN}	mW	20
R_L	Ω	510
α	-	0.1

Table 6: Fixed Parameters

For each of the diodes, the frequency, f, of the input signal has been varied and the corresponding efficiency, η, has been calculated. The data are as follows:

f (GHz)	Efficiency, η (%)				
	HSMS-282x	**HSMS-285x**	**HSMS-286x**	**SMS-7621**	**SMS-7630**
0.90	65.2	76.2	78.4	80.2	80.2
2.00	37.1	62.8	74.3	77.6	72.6
2.45	28.7	56.6	71.9	76.1	68.5
3.00	21.0	49.2	68.6	73.9	63.2

4.45	9.84	33.1	58.6	68.1	49.1
5.00	7.56	28.4	54.7	65.1	44.3
5.80	5.26	22.9	49.2	59.4	38.0

Table 7: Efficiency results from mathematical analysis

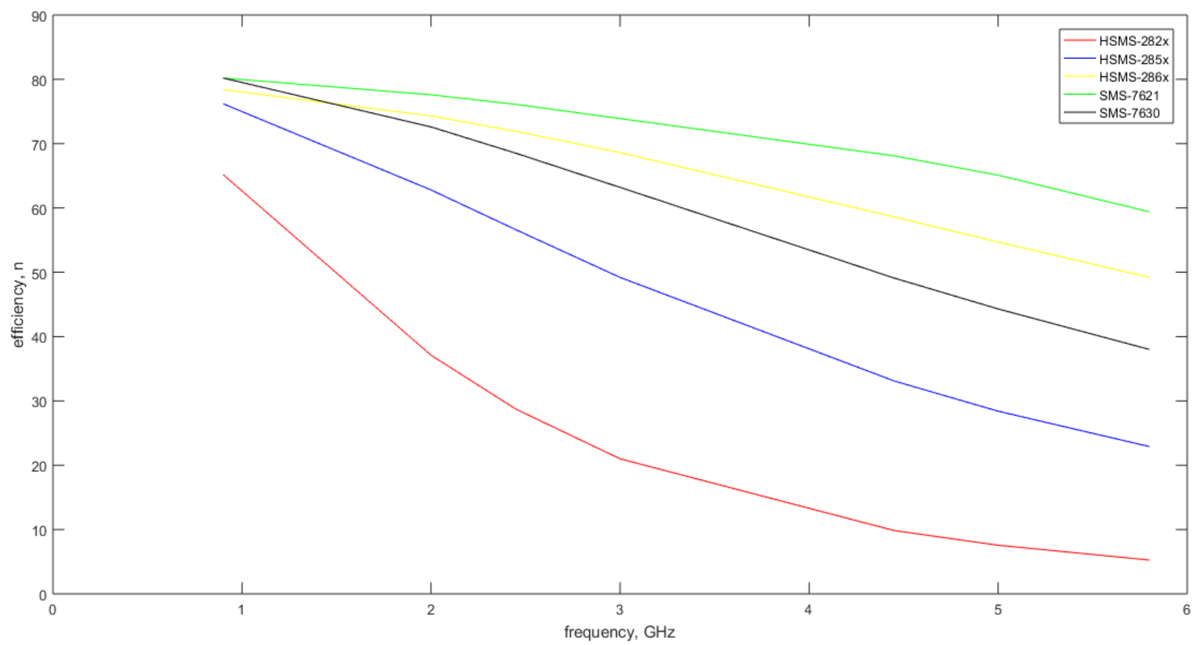

Fig. 6.14 Calculated efficiency of multiple diode models for different frequencies of input power

Fig. 6.14 illustrates how the diode efficiency varies with changing frequency of the input signal. The frequency can be changed since the range for microwave varies from 900MHz to 300GHz. The general trend shows a decrease in diode efficiency with an increase in frequency. The 900MHz frequency value has been chosen since microwave starts from 900MHz, the values 2.45GHz [22] and 5.80GHz [26] have been taken into consideration since at these frequencies high rectification efficiencies had been obtained and the values 2GHz and 3GHz have been chosen to obtain smooth curves. It is quite evident from the plots that SMS-7621 and HSMS-286x are the most suitable diodes since these have the least variation in their respective efficiency trends. For these diodes, the decrease in efficiency is the lowest with an increase in frequency and, also, have the highest values of efficiencies compared to other diodes. From the table it can be observed that at 900MHz, SMS-7621 and HSMS-286x have the maximum values for efficiency compared to the other diodes and not only that, they also have the highest values at 5.80GHz. Two best diodes have been discussed since other parameters have to be considered, along with the change in frequency, to pick the most suitable one. This comparison analysis helps us to choose the best possible diode, with minimum loss, for optimum conversion output.

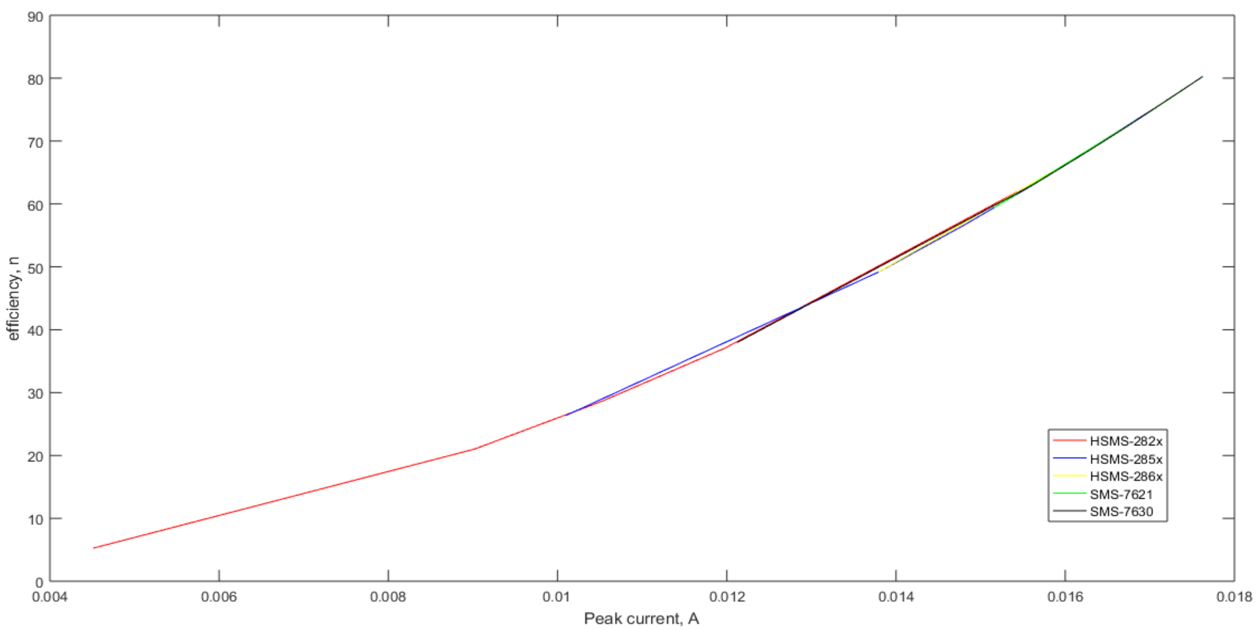

Fig. 6.15 Simulation results of diode efficiency with increasing inverse peak current

Fig. 6.15. illustrates the change in diode efficiency with increasing peak current of the diode. As the frequency in increased, the value of peak current decreases and, hence, the efficiency also falls. The peak current and frequency have an inverse relationship which can be deduced from the extensive efficiency calculations and, thus, when the frequency is increased, the peak current falls and so does the diode conversion efficiency.

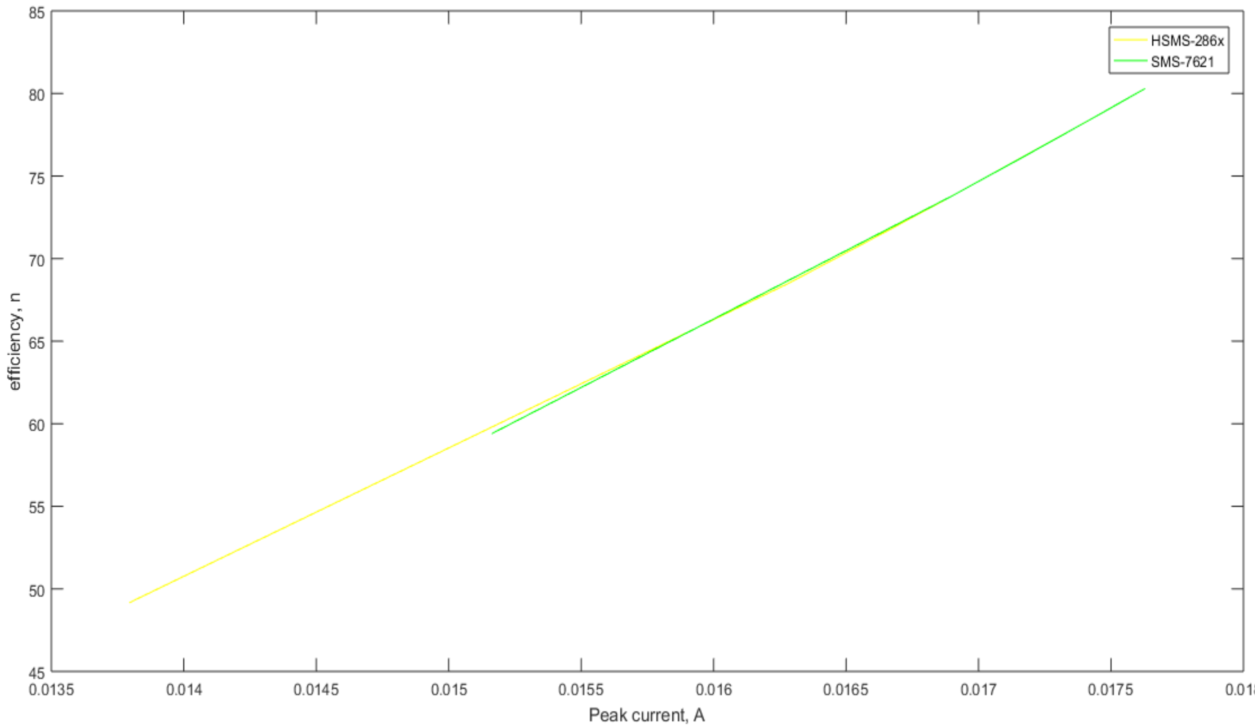

Fig. 6.16 Simulation results of diode efficiency with increasing inverse peak current of the two best models

Fig. 6.16 shows the efficiency trend of the two most suitable diodes selected and discussed from Fig. 6.14, for a better understanding. The decreasing efficiency trend is much clearer in this plot. Therefore, Fig. 6.14 and Fig. 6.15 combined confirms and validates the trend in diode efficiency with an increasing frequency of the input signal which is, as the frequency increases, the efficiency falls.

From the above two comparative analyses it can be concluded that HSMS-286x and SMS-7621 can be stated as the most suitable diodes for maximum rectification since both of their efficiencies increase with an increase in input power level and have comparatively high values when the frequencies were increased although the efficiencies had fallen eventually. However, to select the most suitable diode, one needs to make a balance between the effects of the two variables, input power and frequency, to get maximum rectification efficiency and, also, needs select as per the consumer requirements.

Calculation:

The following is the extensive efficiency calculation for a diode with the given parameters at a frequency of 900MHz.

Diode Model: HSMS-286x

C_{jo} = 0.18pf

R_S = 6Ω

V_{bi} = 0.65V

P_{IN} = 20mW

R_L = 510Ω

α = 0.1

Starting with,

$$R_L = \frac{-2I_P R_S - \pi V_{bi} + \pi V_P}{2I_P}$$

=> $510 = \frac{-12*I_P - 0.65*\pi + \pi * V_P}{2*I_P}$

From equation (6.9.14),

=> $V_P = \frac{1032}{\pi} I_P + 0.65$

However, (6.9.15) states

$$= \frac{I_P(-12I_P - 0.65\pi + \pi V_P)}{2\pi^2(10 \times 10^{-3})}$$

Substituting equation (6.9.14) into (6.9.15) we get equation (6.9.16)

$$\eta = \frac{1020 * I_P^2}{0.02 * \pi^2}$$

But From equation (6.8.13),

$$\eta = \frac{2I_P(-2I_P R_S - \pi V_{bi} + \pi V_P)}{2I_P(-2I_P R_S - \pi V_{bi} + \pi V_P) + \pi I_P(I_P \pi R_S + 4V_{bi}) + \frac{16\pi^2 f^2 C_j^2 V_P^2 R_S}{\alpha}}$$

Additionally, as in equation (6.9.18) below,

$$= (2.4866 \times 10^{-4})V_P^2$$

Substituting equation (6.9.14) into equation (6.9.18) we get

$$(2.4866 \times 10^{-4})V_P^2 = 2.4866 \times 10^{-4}\left(\frac{1032}{\pi} I_P + 0.65\right)^2$$

Now substituting equation (6.9.19) into equation (6.8.13) we get,

$$\eta = \frac{2 * I_P(-12 * I_P - 0.65\pi + \pi * V_P)}{2 * I_P(-12 * I_P - 0.65\pi + \pi * V_P) + \pi * I_P(6\pi I_P + 2.6) + 2.4866 * 10^{-4} * (\frac{1032}{\pi} I_P + 0.65)^2}$$

$$= \frac{2040 I_P^2)}{(2126.051)I_P^2 + (8.274)I_P + (1.0506 \times 10^{-4})} \quad (6.9.21)$$

Now, substituting equation (6.9.16) into equation (6.9.21) we get,

$$2126.05 * I_P^2 + 8.274 * I_P - 0.789 = 0$$

Solving this we get,

$I_P = 0.017422$

Substituting this value into equation (6.9.16) gives us,

η = 0.784 = 78.4%

Similar calculations have been carried out for different input frequency values to obtain the respective efficiencies for different diode models.

The equations that have been used for diode efficiency calculations are as follows:

$$R_L = \frac{-2I_P R_S - \pi V_{bi} + \pi V_P}{2I_P}$$

$$\eta = \frac{P_{OUT}}{P_{IN}} = \frac{I_P(-2I_P R_S - \pi V_{bi} + \pi V_P)}{2\pi^2 P_{IN}}$$

$$\eta = \frac{P_{OUT}}{P_{IN}} = \frac{2I_P(-2I_P R_S - \pi V_{bi} + \pi V_P)}{2I_P(-2I_P R_S - \pi V_{bi} + \pi V_P) + \pi I_P(I_P \pi R_S + 4V_{bi}) + \frac{16\pi^2 f^2 C_j^2 V_P^2 R_S}{\alpha}}$$

6.10 DC Combiner and Output Load

As mentioned earlier in Section (6.2), using a rectenna array improves the absorption of input microwave signals which in turn increases the rectification efficiency. After the individual input power has been rectified, the DC output needs to be combined before being fed into a load. This is where a DC combiner is required. In general, a DC combiner box is used to add up the several outputs of the individual rectifier circuits. Finally, a resistive load is used to carry out experiments where the output of the DC combiner is directly fed into. The output load also has an impact on the total impedance, Z, as discussed in Section (6.5) and needs to be chosen carefully.

Chapter 7 Combined system

7.1 Overall design of the system

The entire system could not be designed entirely due to limited resources and time. Nonetheless, key points of the wireless transmission system were tackled in this work. These include *Chaotic Waveforms, Antenna, Channel Efficiency and Rectenna.* First of all, we suggest that the system be fed with a chaotic waveform to transmit the power, then for channel efficiency, we propose using a higher transmission frequency, for the case of the antennas used, we suggest the non-uniform antenna array especially in the receiving end. Finally, for the rectenna, the class F rectifier is proposed to be used.

7.1.1 Channel efficiency

For better efficiency, as discussed in Chapter 4 for better efficiency, a higher frequency signal should be used. However, the frequency can-not be arbitrarily increased to a certain value. With arguments given in the channel efficiency chapter, one of which is, as we increase the frequency, at a certain range, the penetration of the signal reduces due to having high power thus more reactions being possible along the transmission line

7.1.2 Antenna

As deduced in Chapter 3, the non-uniform antenna array promises to provide better stability and consistency for a better output. The uniform array has a higher gain and directivity according to simulation results got in HFSS thus should be a better option for use in the transmitter side.

7.1.3 Waveforms

The choice for waveform to be used in the signal is the chaotic waveforms since it has higher average number of peaks thus will be able to turn on the diode for a little longer even if the average power of the signal is low. As a result, the efficiency at the rectification end will be better. In case the chaotic waveform is not achieved, the best possible alternative is the white noise signal since it has a higher peak to average power ratio.

7.1.4 Rectenna

The research on rectenna in this work mainly focused on three main parts which include the significance of using a rectenna array, choosing class-F rectifier over the traditional single-shunt rectifier and the comprehensive study on diode efficiency. Firstly, opting for an array of rectenna helps to control the amount of input power into the rectifier circuit. Having a division of array allows more power to get absorbed which directly affects the rectifier efficiency. Moreover, this configuration allows the level of input power to be limited which would otherwise affect the diode's low power working region. Secondly, the class-F rectifier has a huge contribution in the rectifier efficiency since it has an upgraded impedance matching network which can be altered to obtain optimum output and it has an additional RF choke which helps to terminate higher harmonics. Last but not the least, this work has a contribution on diode efficiency comparison. In the channel efficiency chapter, it has been seen that as we increase the efficiency of the transmitted wave signal, channel efficiency rises, keeping the distance between the antennas constant, higher the frequency higher is the channel efficiency. Our main work in the rectifier circuit was diode efficiency comparison based on changes in frequency of input signal. From the simulated values it was observed that higher the frequency of the input signal, lower is the conversion efficiency and the comparison was done for multiple diodes. From this it can be concluded that a balance has to be obtained between the channel efficiency and the rectifier efficiency while selecting the most suitable frequency for optimum efficiency. Referring to the system block diagram, high frequency microwave is transmitted through the wireless channel after which it directly enters the rectenna to be rectified into DC signal. Thus, it is extremely crucial to select the best possible frequency which will give optimum efficiency for both the channel and the rectifier end.

Chapter 8 Conclusion

8.1 Summary

This papers work concentrated on improving efficiency of a wireless power transmission system by improving the antenna part using non-uniform rectenna array and a uniform array for transmitter part, using a high frequency to reduce the channel's effects on the transmitted power, use of chaotic waveform to help improve the RF to DC conversion during rectification and finally the class F rectifier in the receiving end. One of the notable observations is that there is no sovereignty in using PAPR in determining which signal should be chosen since a single peak may give one signal a higher peak to average power ratio however another signal may have more peaks that are above the threshold value even if they are not as high as the single peak in their counterpart. Another great observation is that the non-uniform array especially that of both rectangular and circular patches combined provides a better consistency as the parameters of the system dimensions change thus may not cause great chaos if a small error or in-accuracy is done in the construction of the antenna

8.2 Future work

Future work to be done to integrate all the four proposed techniques into one system and investigate how the overall efficiency of the system is affected.

References

[1] . S. Mohammad, H. Saman and . A. Mohammad, "Wireless Power Transmission Trends," in *3rd INTERNATIONAL CONFERENCE ON INFORMATICS, ELECTRONICS & VISION 2014*, 2014.

[2] A. . l. Muhammad , A. A. Syed and . A. Muhammad, "Wireless Power Transfer Using Microwaves At 2.45 GHz ISM Band," in *Intemational Bhurban Conference on Applied Sciences & Technology*, Islamabad, Pakistan, 2009.

[3] . C. A and . G. A, "Optimal Waveforms for Efficient Wireless Power Transmission," *IEEE MICROWAVE AND WIRELESS COMPONENTS LETTERS,* vol. 24, no. 05, 2014.

[4] . C. Ana and G. Apostolos, "Improving Wireless Power Transmission Efficiency Using Chaotic Waveforms," in *2012 IEEE/MTT-S International Microwave Symposium Digest*, Montreal, QC, Canada, 2012.

[5] K. Ryosuke , . S. Tomohiro and . S. Koichi, "A Study of Rectenna Receiving Area Division for Microwave Wireless Power Transfer System," in *Proceedings of 2017 Asia Pacific Microwave Conference*, 2017.

[6] Y. A-Min , A. Nicola and R. Paolo , "A novel planar frequency diverse array design approach for far-field wireless power transmission," in *IEEE International Symposium on Antennas and Propagation & USNC/URSI National Radio Science Meeting*, San Diego, CA, USA , 2017.

[7] W. Chia-Hao , P. Guan-Pu , H. Hao-Ming and S. Jwo-Shiun , "A 2.45-GHz planar array antenna with harmonic suppression for wireless power transmission applications," in *IEEE Wireless Power Transfer Conference (WPTC)*, Taipei, Taiwan , 2017.

[8] Z. Hong-Yin , . Z. Fu-Shun, Z. Fan , S. Fu-Kun and X. Guo-Jun , "High-Power Array Antenna Based on Phase-Adjustable Array Element for Wireless Power Transmission," *IEEE Antennas and Wireless Propagation Letters,* vol. 16, pp. 2249 - 2253, 2017.

[9] K. Jin-Hyoung, Y. Hyun-Yong and C. Cheolung, "Efficiency enhancement using beam forming array antenna for microwave-based wireless energy transfer," in *2014 IEEE Wireless Power Transfer Conference*, Jeju, South Korea, 2014.

[10] . E. Mauro, A. Waleed A. and . G. Anthony, "Long slot array for wireless power transmissio," in *11th European Conference on Antennas and Propagation (EUCAP)*, Paris, France, 2017.

[11] N. Shinohara, "Rectennas for microwave power transmission," *IEICE Electronics Express,* vol. 10, no. 21, 2013.

[12] K. Ryosuke, S. Tomohiro and S. Koichi , "A study of rectenna receiving area division for microwave wireless power transfer system," in *IEEE Asia Pacific Microwave Conference (APMC)*, Kuala Lumpar, Malaysia , 2017.

[13] W. Shaopeng and H. Kama , "Methods for Improving the Transmission-Conversion Efficiency From Transmitting Antenna to Rectenna Array in Microwave Power Transmission," *IEEE ANTENNAS AND WIRELESS PROPAGATION LETTERS,* vol. 17, no. 4, pp. 538 - 542, 2018.

[14] C. A. Balanis, Antenna Theory: Analysis and Design, Hoboken, New Jersey: John Wiley & Sons, Inc., 2005.

[15] K. Mohsen , . T. Rahim , R. T. A and K. M. R. , "Design of Phased Arrays of Series-Fed Patch Antennas With Reduced Number of the Controllers for 28-GHz mm-Wave Applications," *IEEE Antennas and Wireless Propagation Letters,* vol. 15, pp. 1305 - 1308, 2015 .

[16] F. H. T, " A Note on a Simple Transmission Formula," *Proc. IRE,* vol. 34, no. 5, pp. 254-256, 1946.

[17] . K. Ioannis, . T. Stelios, . N. Symeon, D. W. K. N. Gan and S. Robert , "Simultaneous wireless information and power transfer in modern communication systems," *: IEEE Communications Magazine,* vol. 52, no. 11, pp. 104 - 110, November 2014.

[18] "Learning about Electronics," c 2018. [Online]. Available: http://www.learningaboutelectronics.com/Articles/Schottky-diode.php. [Accessed 20 4 2019].

[19] M. Rouse, "TechTarget," September 2016. [Online]. Available: https://searchnetworking.techtarget.com/definition/orthogonal-frequency-division-multiplexing. [Accessed 20 April 2019].

[20] "Sunny Classroom," October 2018. [Online]. Available: https://www.youtube.com/watch?v=KCHO7zlU25Q&feature=share&fbclid=IwAR1Iuu1MQX7nE2zrVR7V8TeVr7bsz-iC6BRfiA8o3e-uAybF6Cdc9JSYvZs. [Accessed 20 April 2019].

[21] D. Hien , R. John C and M. Thomas E. , "Chaotic dynamics of a frequency-modulated microwave oscillator," *Chaos: An Interdisciplinary Journal of Nonlinear Science,* vol. 23, no. 1, 2013.

[22] C. Doan Huu and D. Bach Gia , "Investigation of Rectifier Circuit Configurations for Microwave Power Transmission System Operating at S Band," *International Journal of Electrical and Computer Engineering (IJECE),* vol. 5, no. 5, p. 967~974, October 2015.

[23] S. Chaoyun , H. Yi , Z. Jiafeng , C. Paul , Y. Sheng , X. Qian and F. Zhouxiang , "Matching Network Elimination in Broadband Rectennas for High-Efficiency Wireless Power Transfer and Energy Harvesting," *IEEE Transactions on Industrial Electronics,* vol. 64, no. 5, pp. 3950 - 3961, May 2017.

[24] G. Jiapin , Z. Hongxian and Z. Xinen , "Theoretical Analysis of RF-DC Conversion Efficiency for Class-F Rectifiers," *IEEE Transactions on Microwave Theory and Techniques,* vol. 64, no. 4, pp. 977 - 985, April 2014.

[25] P. M. Masud, "A methodology for designing 2.45 GHz wireless rectenna system utilizing Dickson Charge Pump with Optimized Power Efficiency," UWSpace, Waterloo, Ontario, Canada, 2013.

[26] A. Amal , S. Mohamed Adel , B. Larbi , . A. Anouar and Y. Nourdin , "Enhanced RF Energy Harvester for Power Efficient Internet-of-Things Wireless Sensors," in *2018 6th International Conference on Multimedia Computing and Systems (ICMCS)*, Rabat, Morocco , May 2018 .

[27] Y. Xiaodong , G. Wen and S. Hucheng , "Optimum Design of Wireless Power Transmission System Using Microstrip Patch Antenna Arrays," *IEEE Antennas and Wireless Propagation Letters ,* vol. 16, pp. 1824 - 1827, 2017.

[28] P. Nayeri, "Focused antenna arrays for wireless power transfer applications," in *International Applied Computational Electromagnetics Society Symposium (ACES)*, Denver, CO, USA , 2018.

[29] A. Alexander , Q. Roberto , C. Peng , A. Sattam , T. Paul J. and L. Jonathan , "Analysis of Highly Efficient Self-Synchronous Class-F Microwave Rectifiers Using Waveform Engineering," in *48th European Microwave Conference (EuMC)*, Madrid, Spain , 2018.

[30] A. Sadegh and J. Thomas , "Power-Efficiency Characteristics of Class-F and Inverse Class-F Synchronous Rectifiers," *IEEE TRANSACTIONS ON MICROWAVE THEORY AND TECHNIQUES,* vol. 64, no. 12, pp. 4740 - 4751, 2016.

[31] A. Collado and A. Georgiadis, "Optimal Waveforms for Efficient Wireless Power Transmission," *IEEE Microwave and Wireless Components Letters,* vol. 24, no. 5, pp. 354 - 356, 2014.

Appendix A

Code used for signals.

White noise signal

%the code is given below

```
clear all; clc; close all;
L=3000; %Sample length for the random signal
mu=0;
sigma=2;
X=sigma*randn(L,1)+mu;

figure();
subplot(2,1,1)
plot(X);
title(['White noise : \mu_x=',num2str(mu),' \sigma^2=',num2str(sigma^2)])
xlabel('Samples')
ylabel('Sample Values')
grid on;
v = rms(X)
v_peak = max(X)
```